NTNU

Norwegian University of
Science and Technology

A Density Functional Theory Study of Hydrogen Transfer and Rotational Barriers in Vitamin E-like Molecules

Ragnhild Aurlien

Teacher Education with Master of Science
Submission date: June 2011
Supervisor: Jon Andreas Støvneng, IFY

Norwegian University of Science and Technology
Department of Physics

Abstract

A study of the antioxidant property of two vitamin E simplifications with density functional theory has been done. In one of the simplifications the phytyl tail and the methyl group on the heterocyclic ring in vitamin E is replaced by two hydrogen atoms, simplification **A**. In the other simplification the heterocyclic ring is replaced by two hydrogen atoms, simplification **B**. Three main investigations have been done; rotation of the hydroxyl group on the different isoforms of the two simplifications, hydrogen transfers from the α-isoform of the simplifications to three different radicals $^{\bullet}OOH$, $^{\bullet}OOCH_3$, and $^{\bullet}OOC_2H_5$, and a rotation of the hydroxyl group with a hydrogen bond to $^{\bullet}OOH$ and $^{\bullet}OOCH_3$ for simplification **B**. The BLYP exchange correlation functional is found to underestimate hydrogen transfer energy barriers, which is improved with the B3LYP functional. This problem did not occur for the rotation of the hydroxyl group. The energy barriers for the rotation of the hydroxyl group is found to be smallest for the α-isoform, and simplification **A** gives lower rotational barriers than simplification **B**. Simplification **A** also results in smaller energy barriers for hydrogen transfers. The hydrogen transfer to $^{\bullet}OOC_2H_5$ with the B3LYP functional resulted in hydrogen barriers of 0,411 eV for simplification **B** and 0,231 eV for simplification **A**. Thus simplification **B** is found to be less reactive than simplification **A**, which is explained by the electron donating property of the heterocyclic ring not included in simplification **B**. Since simplification **B** is less reactive than simplification **A**, it is concluded to be a poorer antioxidant than simplification **A**, and a poor model for vitamin E.

Acknowledgement

This thesis has been written as a final thesis for my study at the Department of Physics at the Norwegian University of Science and Technology (NTNU) in Trondheim. The thesis has been written within one semester, from January to June 2011.

I would like to thank my supervisor Jon Andreas Støvneng, and Thor Bernt Melø for much appreciated help during the semester. I would also like to give a big thank to Helene Hauge and Tor Ingve Aamodt for motivation, help and good mood in the study hall through this final stage of the study. Finally, I would like to thank Gudrun, Erling, Erland, Thomas, Jesper, Bell, Igor and Gauss for helping me with my calculations.

Contents

Chapter 1

Introduction

1.1 Vitamin E

In 1920 Mattill and Conklin started investigating whether milk was a nutrition source that could give sufficient and necessary nutrition throughout life or not [1]. This study of milk as a "perfect food" was the start of the nutrition study eventually leading to the finding of vitamin E and the classification of its functions. Mattill and Conklin found that with a diet of mainly milk, the growth of rats was normal, but they were sterile. After more studies, it was concluded by Evans and Bishop that these purified diets lacked some substance that was essential for reproduction, but not for normal growth [1]. The name *vitamin E* was suggested, since vitamin A, B, C and D were already known. It was also called the antisterility vitamin. In 1936, Evans and others gave the substance the name *tocopherol*, derived from the ancient Greek words *phero* meaning "to bring", and *tocos* meaning "childbirth" [1].

Today vitamin E is defined as different isoforms of tocopherols and tocotrienols [2]. vitamin E can be found for example in nuts, seeds and vegetable oils [3]. Green leafy vegetables are also good sources of vitamin E. A grown up person needs about 15 mg of vitamin E daily, and vitamin E deficiency is rare [3].

1.1.1 Structure

There are all together eight naturally occurring isoforms of vitamin E: α-, β-, γ-, and δ-tocopherols and α-, β-, γ-, and δ-tocotrienols [4]. All the isoforms consist of a chroman head with a phytyl tail [2]. The head consists of two rings, one heterocyclic ring consisting of carbon and one oxygen atom, and one phenolic ring with a hydroxyl group and one, two or three methyl groups. The tocopherols and the tocotrienols differ only in their tail.

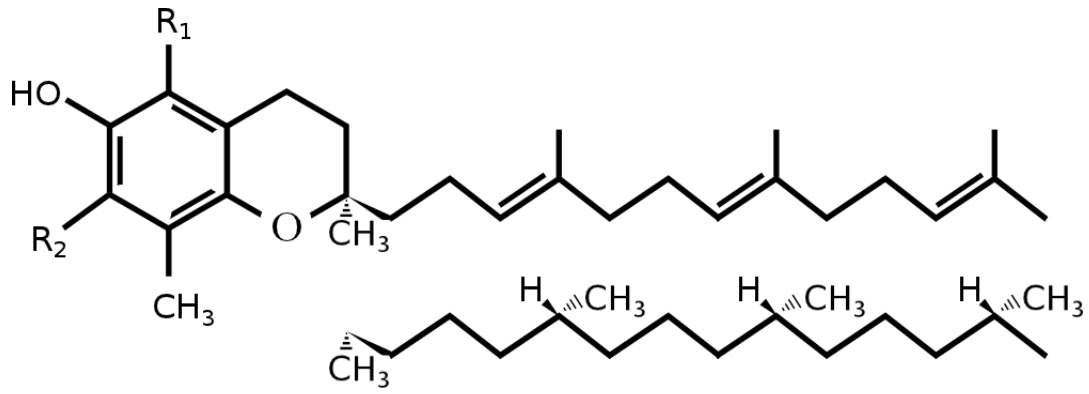

Figure 1.1: *Molecular structure of vitamin E with its two different side chains. The top chain is tocotrienol isoprenoid side chain, and the bottom one is tocopherol phytyl side chain. Based on Fig. 1 in [4].*

The molecular structure of vitamin E can be seen in Fig. (1.1). Here the vitamin is shown with the two different side chains; the top one is tocotrienol isoprenoid side chain, and the bottom one is tocopherol phytyl side chain [4]. The α-, β-, γ-, and δ-isoforms only differ in the number and placement of the methyl groups. The α-isoform has three methyl groups, the β- and γ-isoforms have two, and δ only one. The placement leading to the different isoforms can be seen in Table 1.1.

Table 1.1: *Isoforms of vitamin E [4]. Substituents R1 and R2 are shown in Fig. (1.1)*

	R1	R2
α	CH_3	CH_3
β	CH_3	H
γ	H	CH_3
δ	H	H

The human body can absorb all forms of vitamin E [4]. The recommended intake of vitamin E mentioned above is nevertheless based only on the need for α-tocopherol.

This is because the human body only maintains α-tocopherol, and the uptake of it is also preferred. α-tocopherol is the most biologically active isoform [4, 5, 6, 7].

Vitamin E is the least understood vitamin, even though it is almost 90 years since it was discovered [8]. The functions of vitamin E are mainly mediated by its antioxidant action and its action as a membrane stabilizer [7], it is even suggested that the primary function of α-tocopherol is to act as an antioxidant [9]. Vitamin E is considered to be a very important antioxidant in the human body, and it is claimed that "*vitamin E is the major (and possibly only) lipid-soluble, chain-breaking antioxidant in human blood*" [10, p. 197]. Below the antioxidant property of vitamin E will be investigated.

1.1.2 The antioxidant property of vitamin E

A redox reaction is a reaction where a molecule, atom or ion obtains an increased oxidation number, while another obtains a decreased oxidation number. The first case is called an oxidation, and the latter a reduction; together a redox reaction. This can for instance happen if a hydrogen atom is transferred from molecule A to B, and A is then oxidized, and B is reduced.

This reaction can produce a free radical, denoted $R^{\bullet}$. In biological material a radical can be created by heat, light, by a simple electron transfer, or by other external factors. A radical is a very reactive molecule [10]. The creation of a radical is thus the beginning of a chain reaction that can have disastrous consequences. It can cause damage on biological molecules such as DNA, proteins, carbohydrates and lipids, leading to a variety of diseases such as cancer, arthritis, aging and heart diseas [7]. An antioxidant can stop this unfortunate chain reaction, and thus protect organic materials from oxidation. To stop the chain reaction, the antioxidant can donate a hydrogen atom to the radical. Although the antioxidant then itself becomes a radical, it is much more stable, and does not, in general, continue the chain.

Vitamin E is as mentioned an antioxidant, and is protecting biological membranes from oxidation. It is lipophilic, and can therefore be located in biological membranes. A biological membrane consists of a lipid bilayer, and protects the cell which it surrounds. A cross section of a lipid bilayer can be seen in Fig. (1.2), with vitamin E included. This is only a model, since the real location and arrangement of vitamin E in biological membranes is unknown [7]. Oxidation of the lipids making up the membrane around a cell may cause the cell to be damaged.

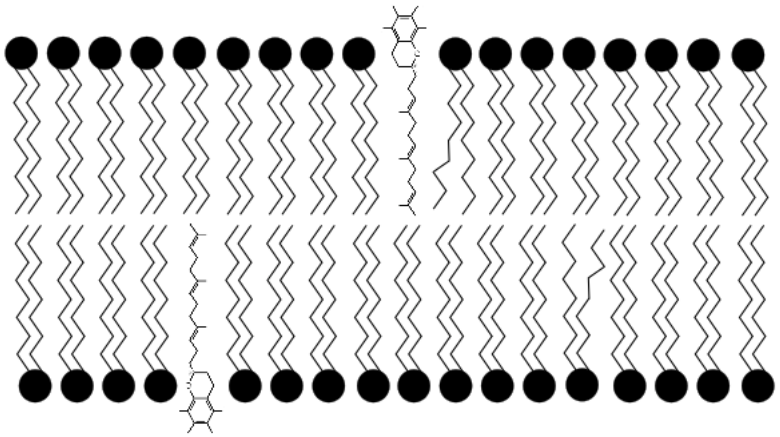

Figure 1.2: *A cross section of a segment of a lipid bilayer with vitamin E. The •-symbol represents a lipid head. The lipids with an unhomogeneous tail, are unsaturated lipids. Based on Fig. 8 in [7], Fig. 5b in [11] and Fig. 1 in [12].*

If a membrane lipid becomes oxidized, vitamin E can donate the hydrogen on the hydroxyl group to stop the oxidation chain reaction.

The oxidizing chain reaction consists of mainly three steps [13],

I: Initiation

$$RH \rightarrow R^{\bullet} + H \tag{1.1}$$

II: Addition of O_2

$$R^{\bullet} + O_2 \rightarrow ROO^{\bullet} \tag{1.2}$$

III: Hydrogen atom exchange

$$ROO^{\bullet} + RH \rightarrow ROOH + R^{\bullet} \tag{1.3}$$

where RH and $R^{\bullet}$ denotes the lipid and the lipid radical, respectively. In the first reaction a free radical is created, and is what starts the whole reaction. Reaction 1.2 and 1.3 then forms a chain reaction that converts many lipid molecules into lipid hydroperoxide (ROOH) [13]. Reaction 1.2 is very fast, but reaction 1.3 is slower. This chain reaction continues until two $ROO^{\bullet}$-radicals react with each other creating nonradical products [9]. However, in the presence of a chain-breaking antioxidant, i.e. vitamin E, another reaction will terminate the chain reaction [13]:

IV: Donation of hydrogen from antioxidant to the free radical

$$ArOH + ROO^{\bullet} \rightarrow ArO^{\bullet} + ROOH \tag{1.4}$$

where ArOH denotes the phenolic antioxidant, i.e. vitamin E. This reaction happens faster than reaction 1.3, and thus breaks the oxidizing chain [13]. This reaction chain is also outlined in Fig. (1.3).

The breaking of the chain can happen in two other mechanisms than the hydrogen atom transfer (HAT) shown in Eq. (1.4). These are sequential proton-loss-electron-transfer (SPLET) and stepwise electron-transfer-proton-transfer (ET-PT), but they all end up with the same result [14]. The HAT does not include charge separation, and is therefore preferred in non-polar solvents, i.e. lipids. The two other mechanisms do imply charge separation, and is therefor favored in polar media. Zhang and Ji [14] also claim that HAT and SPLET are more probable than ET-PT.

One can see from Eq. (1.4) that vitamin E ends up as a radical after donating the hydrogen atom to the lipid radical. Although it is far less reactive than the free radical, it still is a radical. If the concentration of the vitamin E radical becomes too high, the reverse reaction can occur, and the vitamin can oxidize other molecules, creating free radicals [8]. This is avoided by vitamin C, ascorbate. vitamin C can reduce and thus regenerate vitamin E to its active antioxidant form [15], which adds a fifth step to the above chain reaction:

V: Regeneration of vitamin E from vitamin C, ascorbate

$$(ArO^{\bullet})_{lipid} + (AH^{-})_{aq} \rightarrow (ArOH)_{lipid} + (A^{-})_{aq} \tag{1.5}$$

where AH^{-} denotes ascorbate. This reaction happens in the water-lipid interface. Vitamin C is not able to reduce the lipid radicals directly, since it is water soluble [15]. It is widely accepted that vitamin C, ascorbate, plays a role in reducing vitamin E, but proofs of this in vivo is scarce [8]. Ubiquinol ($Q_{10}H_2$) can also scavenge the vitamin E radical, but the ubiquinol levels in tissue are often too low to contribute much [8]. Studies indicate that the effect of vitamin E and vitamin C are additive [10].

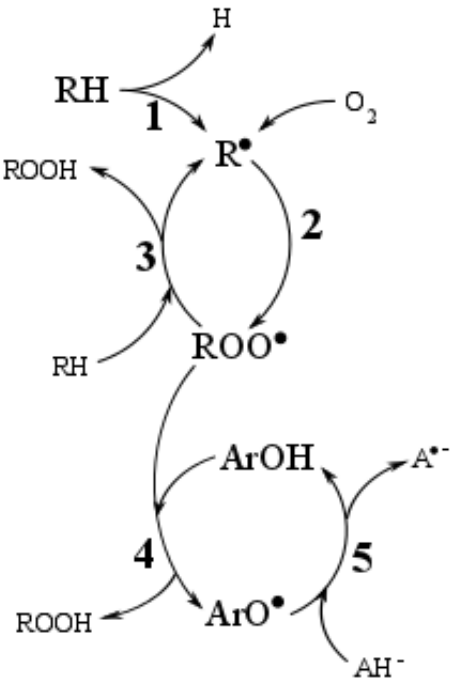

Figure 1.3: *A schematic overview of the radical ($R^{\bullet}$) chain reaction, the breaking of this by vitamin E (ArOH), and the regeneration of vitamin E by vitamin C (AH^{-}). The numbers denotes the five steps in Eq. 1.1-1.5. Based on Eq. (1-4) in [13] and Fig. 2 in [7].*

1.2 Our contribution

Our main focus in this thesis has been the antioxidant property of vitamin E, i.e. the hydrogen atom transfer shown in Eq. (1.4). The computational method used to study this hydrogen transfer is a quantum mechanical method called density functional theory (DFT), using a program called Amsterdam Density Functional (ADF). We have used two simplified vitamin E-like molecules in our computations, and one of our goals has been to investigate how the heterocyclic ring effects the antioxidant activity of vitamin E. We also studied the activation energy, or the barrier height, for the hydrogen transfer, i.e. the energy barrier needed to be overcome to start the hydrogen transfer from vitamin E to a radical.

Our initial approach, however, was to study the rotation of the hydroxyl group in vitamin E. Other studies [16, 17, 18] of this rotation in connection with hydrogen transfers and electron transfers has been done. These studies claims that the

rotation of the hydroxyl group on phenol rotates with a frequency of 10^{13} Hz with a activation barrier less than 3 kcal/mol (0,13 eV). The antioxidant activity and how it happens depends on the orientation of the hydroxyl group. We therefor wanted to investigate this further, i.e. how large the energy barrier were for different isoforms and simplifications of vitamin E, and how large the hydrogen transfer energy barriers where depending on the C-C-O-H dihedral angle. However, during the process, the focus was moved towards the above mentioned hydrogen transfer reactions. Although the focus changed, we did study the rotation barriers for the hydroxyl group, and the same rotation when the hydroxyl group was attached to a radical.

When doing DFT computations, a lot of options have to be specified. (A more detailed introduction to DFT can be found in chapter 2). One of these options is which exchange correlation functional is to be used. BLYP, B3LYP and BHandHLYP are three such functionals, where BLYP is a so-called generalized gradient approximation (GGA) functional, and B3LYP and BHandHLYP are so-called hybrid functionals. One shortcoming with the DFT method, is that barrier heights are underestimated with many exchange-correlation functionals [19]. The GGA functionals has this problem, but the results are improved with the hybrid functionals. Still, in a database with 76 known barrier heights, B3LYP made an average underestimation of 4.4 kcal/mol (0.19 eV) [19].

A lot of other studies confirm that the exchange correlation functional underestimates the barrier heights. Baker, Andzelm, Muir and Taylor carried out a hydrogen transfer calculation with DFT for the reaction $OH+H_2 \rightarrow H_2O+H$ [20]. They performed the calculation with a lot of different exchange correlation functionals with the program GAUSSIAN 90. With BLYP they actually found a negative energy barrier for the hydrogen transfer, and the only DFT functionals that gave a correct barrier height were the hybrid functionals.

Nguyen, Creve and Vanquickenborne have also done some studies on the reliability of different functionals [21]. In their study, Nguyen et al. studied hydrogen addition to different radicals. DFT seems to have problems in reproducing long distance interactions, and underestimates energy barriers. The three DFT functionals used were BLYP, B3LYP and BHandHLYP, where BLYP resulted in the smallest energy barriers, B3LYP in a bigger one and BHandHLYP in the largest one.

As we can see in the results from the above studies, certain exchange correlation functionals show problems with prediction of energy barriers. We have therefore

also chosen to study the three different exchange correlation functionals BLYP, B3LYP and BHandHLYP mentioned above for hydrogen transfer reactions from vitamin E. This is to see how large the differences between the results from the different functionals are, and to suggest which functional is the best for this calculation.

The thesis is structured as follows: First the theory used in this thesis is presented. All calculations done are as mentioned based on density functional theory (DFT), a quantum mechanical method, and this method therefore has the main focus in the theory chapter. The first topic is quantum mechanical many particle theory, followed by the Hartree-Fock method, an other quantum mechanical method, before the main part with a brief introduction to DFT. This part includes the Kohn-Sham equations and how to proceed to solve them.

After the theory chapter, the computational method used will be accounted for. All calculations are done using the program Amsterdam Density Functional (ADF), and the program will be presented together with the computational details. An implementation part then follows. This section presents the simplifications of vitamin E that we have used, together with the radicals we have chosen as substitutions for a lipid radical. Hydrogen transfers are also given a special attention since this is our main focus in this thesis. The rest of the chapter includes descriptions of the different calculations done.

The results from the computations are presented and discussed next. First, bonding energies and energies for all single components used are presented for an overview. Then results from the computations described in the implementation section follows. A general discussion is also presented, before conclusions are drawn. Finally future work on this topic are suggested. All the molecules used in this thesis can be found in Appendix A, the geometries for the individual steps on a hydrogen transfer can be found in Appendix B, and molecules showing modes of imaginary frequencies can be found in Appendix C.

Chapter 2

Theory

This chapter presents theory used in this thesis. All calculations are done using a quantum mechanical computational method called density functional theory (DFT). DFT is a method for solving the many-particle problem, which is presented first. Then an approximation for the many-particle wavefunction called the Born-Oppenheimer approximation is presented before the Hartree approximation and the Hartree-Fock method follows. Finally, a brief introduction to DFT is given.

2.1 The Many-Particle Problem

In many quantum mechanical fields, the basic problem is to deal mathematically with the interactions of a large number of particles, for example in a molecule. The goal is often to minimize the energy of the given system. This implies solving the non-relativistic, time-independent Schrödinger equation (SE) to find the ground state energy E:

$$\hat{H}\Psi = E\Psi, \text{or} \tag{2.1}$$

$$\hat{H}|\Psi\rangle = E|\Psi\rangle, \tag{2.2}$$

where he first version of the SE is in normal notation, and the latter is in Dirac notation. If we consider a molecule, it consists of many electrons and nuclei. For such a many particle problem, the Hamiltonian $\hat{H}$ in the SE can be written out accordingly:

$$\hat{H} = \hat{T}_{\text{ion}} + \hat{T}_{\text{el}} + \hat{V}_{\text{ion-ion}} + \hat{V}_{\text{el-el}} + \hat{V}_{\text{ion-el}} \tag{2.3}$$

$$\begin{aligned} &= -\frac{\hbar^2}{2}\sum_{\text{i}}\frac{\nabla^2_{\mathbf{R}_\text{i}}}{m_\text{i}} - \frac{\hbar^2}{2m_\text{e}}\sum_{\text{i}}\nabla^2_{\mathbf{r}_\text{i}} + \frac{1}{8\pi\epsilon_0}\sum_{\text{i}\neq\text{j}}\frac{e^2 Z_\text{i} Z_\text{j}}{|\mathbf{R}_\text{i} - \mathbf{R}_\text{j}|} \\ &+ \frac{1}{8\pi\epsilon_0}\sum_{\text{i}\neq\text{j}}\frac{e^2}{|\mathbf{r}_\text{i} - \mathbf{r}_\text{j}|} - \frac{1}{4\pi\epsilon_0}\sum_{\text{i,j}}\frac{e^2 Z_\text{i}}{|\mathbf{R}_\text{i} - \mathbf{r}_\text{j}|} \end{aligned} \tag{2.4}$$

The first two terms represent the kinetic energy of the ions and electrons, respectively, and the three last terms represent the Coulomb interaction, ion-ion, electron-electron and ion-electron, respectively. $\mathbf{R}_\text{i}$ and $\mathbf{r}_\text{i}$ represent the locations of the ions and the electrons and m_i and m_e represent their masses. Z_i represent the number of protons in ion number i.

Hydrogen-like systems can be solved analytically in closed form using Eq. (2.4), since it consist of only one electron and one proton in the nucleus. As the system expands, the problem becomes complicated. An example of a system we are going to study, is a system consisting of 22 atoms i.e., 22 nuclei and 74 electrons, or a total of 96 particles. We can see from Eq. (2.4) that such a system get vastly complicated and impossible to solve exactly. The advantages of solving this equation are however great, so a lot of approximations are therefore developed to make it solvable. Density functional theory and the Hartree-Fock method is two different quantum mechanical approximate approaches to make Eq. (2.4) solvable. Both are based on the Born-Oppenheimer approximation.

2.2 Born-Oppenheimer approximation

In a molecule, the masses of the nuclei are much greater than the mass of the electron, and the speed of the electrons is thus much greater than the speed of the nuclei [22, p. 158-159]. Any changes in the positions of the nuclei will almost instantaneously lead to changes in the positions of the electrons. The electronic wavefunction therefore depends only on the position of the nuclei, and not on their velocity. The electrons can thus relax to their ground state as if the nuclei were stationary, and this is the Born-Oppenheimer approximation. The energy for the system is then a function of the nuclei positions, and makes up a potential energy surface. The electrons and ions having different time scales implies that the wavefunction of a molecule can be expressed as a product of the electronic and

nuclear components:

$$|\Psi_{\text{tot}}\rangle = |\Psi_{\text{el}}\rangle|\Psi_{\text{ion}}\rangle \tag{2.5}$$

Thus the problem can be thought of as a gas of electrons moving in an external potential. The many particle Hamiltonian in Eq. (2.3) can then be divided into two; an electronic part $\hat{H}_{\text{el}}$ and a nuclei part $\hat{H}_{\text{ion}}$:

$$\hat{H}_{\text{ion}} = \hat{T}_{\text{ion}} + \hat{V}_{\text{ion-ion}} + E_{\text{el}} \tag{2.6}$$

$$\hat{H}_{\text{el}} = \hat{T}_{\text{el}} + \hat{V}_{\text{el-el}} + \hat{V}_{\text{ion-el}} \tag{2.7}$$

with E_{el} being the influence of the electrons on the nuclei due to the Coulomb interaction. The Born-Oppenheimer approximation has divided the problem in two; a nuclei problem and an electronic problem, and it lets us solve the electronic problem independent from the movement of the ions. This leads to an iterative method to solve the SE, as follows [22, p. 158-159]:

1. First, the nuclei are assumed to be stationary at initial positions $\mathbf{R}_{\text{i}}$, and the SE for the electrons is solved, using Eq. (2.7). This results in energy eigenvalues as a function of the nuclear positions, $\epsilon_n(\mathbf{R}_{\text{i}})$.

2. Next, the nuclei are considered. The ground state for the electron problem is used as potential energy together with nuclei-nuclei interactions to relax the nuclei to new, more stable positions, using Eq. (2.6) as the Hamiltonian. If the initial and final positions of the nuclei are the same, this is the solution. If not, restart the process with the new coordinates for the nuclei.

The Born-Oppenheimer approximation makes the solution of the SE easier, as it divides the problem into two. It is however still unsolvable for most systems. More approximations are therefore needed.

2.3 The Hartree approximation

The Hartree approximation was developed in the late 1920's to solve the electronic problem. The method assumes that the probability of finding an electron at a given point in space is independent of the probability of finding another electron at the same point, and that every single electron state is independent of the others [23].

This makes the total Hamiltonian separable, and the electronic wavefunction can then be expressed as the product of single hydrogen atom wavefunctions like

$$|\Psi_{\mathrm{el}}\rangle = \prod_{\mathrm{i}} |\psi_{\mathrm{i}}\rangle, \tag{2.8}$$

the Hartree product.

The method assumes that the electrons do not interact directly with each other, but with a mean potential field from all the other electrons. If electron i is in a one particle orbital $\psi_{\mathrm{i}}(\mathbf{r})$, it will contribute with the charge density $-e|\psi_{\mathrm{i}}(\mathbf{r}_{\mathrm{i}})|^2$ to the total potential felt by all other electrons [22, p. 208-109]. The kth electron will then feel a potential from the nucleus core, and from an average of all the other electrons. The sum over these repulsive and attractive forces is the total potential the kth electron in position $\mathbf{r}_{\mathrm{k}}$ experiences:

$$V(\mathbf{r}_{\mathrm{k}}) = -\frac{Ze^2}{4\pi\epsilon_0 r_{\mathrm{k}}} + \sum_{\mathrm{i}(\neq \mathrm{k})} \int \frac{e^2|\Psi_{\mathrm{i}}(\mathbf{r}_{\mathrm{i}})|^2}{4\pi\epsilon_0|\mathbf{r}_{\mathrm{i}} - \mathbf{r}_{\mathrm{k}}|} d^3 r_{\mathrm{i}} \tag{2.9}$$

where the first part is the potential due to the nuclei, and the second is the average potential from all the other electrons. This potential can be used in Eq. (2.7) to solve the electron part of the SE.

However, we do not know the orbital for electron i. To know which orbital is the better, we can apply the variational principle. It states that an approximate wave function, Ψ^{T}, for the ground state will always yield an upper bound to the exact energy E [23, p. 51-54]. Consequently, the better wavefunction, the lower energy;

$$E \leq \langle \Psi^{\mathrm{T}} | \hat{H} | \Psi^{\mathrm{T}} \rangle. \tag{2.10}$$

The electron problem can then be solved iteratively [22, p. 208-209]: A start potential is chosen, the wavefunctions are calculated, and a new effective potential is calculated from the Z wavefunctions with the lowest energy. This process is repeated until the wavefunctions reproduce themselves.

The Hartree method does satisfy an older version of the Pauli exclusion principle, since all electrons occupy different states. However, it does not satisfy the antisymmetry condition. Electrons are fermions, so the wavefunction must change sign when two electrons are exchanged: $\Psi_{\mathrm{el}}(1,2) = -\Psi_{\mathrm{el}}(2,1)$. The Hartree-Fock method has a solution to this problem.

2.4 The Hartree-Fock method

John Slater introduced the Slater determinant Φ in exchange of the electron states in Eq. (2.8) [24]. This determinant is a determinant of spin orbitals and it satisfies both the Pauli exclusion principle and the antisymmetry principle by construction. Still, the assumption that each electron moves independently of all the others applies. The electrons are assumed to feel the Coulomb repulsion from the average position of all the electrons. In Hartree-Fock (HF) theory, the electron also feels an exchange interaction due to antisymmetrization, but other electron-electron correlations are neglected.

The HF calculations can predict structures and yield results that fit with experiments, but the energetics is not good. The minimal energy for a single Slater determinant is the Hartree-Fock energy, and the difference between the exact energy and the HF energy is called the correlation energy, E_C. This component is due to the many-body interactions.

To correct the HF energy, one can include excited configurations. The more corrections added, the more exact solution. However, when adding corrections, calculation costs are also increased, so the most accurate methods can only be applied to very small systems. We will therefore investigate a method with less computational cost; DFT.

2.5 Density Functional Theory (DFT)

Density functional theory (DFT) is one of the most popular methods for doing calculations on for instance atoms and molecules, and their interactions [25], and it has an excellent performance-to-cost ratio [19]. The main idea in DFT is to use the electron charge density $n(\mathbf{r})$ as a basic variable, instead of the many-electron wave function used in Hartree-Fock theory. DFT has the advantage of being able to solve many problems with high accuracy together with being computationally simple. The scope of this section is to give a short introduction to DFT.

2.5.1 The Hohenberg-Kohn theorems

The entire field of DFT rests upon the idea that there is a relationship between the total electronic energy and the overall electron density, $n(\mathbf{r})$. The basis for this idea was already developed in the 1920's in the Thomas-Fermi method [26, 27], but this method failed to produce any quantitatively impressive results. The theory was brought further by Hohenberg and Kohn in 1964 [28]. The basic idea is that we can use the electron density as a variable instead of the many-electron wave function as in Hartree-Fock theory, and thus consider all the electrons at once instead of using a single-particle approach with single-particle orbitals. Hohenberg and Kohn formulated two theorems [29, p. 10-14]:

Theorem 1. *The ground-state energy from Schrödinger's equation is a unique functional of the electron density;* $E = E[n(\mathbf{r})]$
Theorem 2. *The electron density that minimizes the energy of the overall functional is the true electron density corresponding to the full solution of the Schrödinger equation.*

The proofs of these theorems are *reductio ad absurdum* [28], and will not be given here.

In other words: Instead of solving the Schrödinger equation, one can find the minimum energy for the electron density. With the Schrödinger equation, $3N$ dimensions are needed to find the ground state energy for a system with N particles. With the electron density only three dimensions are needed. This reduces the computational costs and simplifies the problem.

The solution of the SE using the electron Hamiltonian (2.7) can be written as:

$$E = \langle \Psi | \hat{H} | \Psi \rangle = \langle \hat{T} \rangle + \langle \hat{V}_{\text{int}} \rangle + \int V_{\text{ext}}(\mathbf{r}) n(\mathbf{r}) d\mathbf{r} \tag{2.11}$$

where the kinetic energy of the electrons now are denoted $\hat{T}$, the Coulomb interaction between the electrons are denoted V_{int} for internal interactions, and the electron density $n(\mathbf{r})$ are located in an external potential V_{ext} from the nuclei. As a result from the Hohenberg-Kohn theorems, this energy can be written as a unique functional of the electron density,

$$E[n(\mathbf{r})] = T[n(\mathbf{r})] + V_{\text{int}}[n(\mathbf{r})] + U_{\text{ext}}[n(\mathbf{r})] = F[n(\mathbf{r})] + \int V_{\text{ext}}(\mathbf{r}) n(\mathbf{r}) d\mathbf{r}, \tag{2.12}$$

$U_{\text{ext}}[n(\mathbf{r})]$ being the energy due to an external potential (mainly from the nuclei). The functional $F[n(\mathbf{r})]$ is the sum of the kinetic energy of the electrons, $T[n(\mathbf{r})]$,

and the interelectronic interactions, $V_{\text{int}}[n(\mathbf{r})]$. $F[n(\mathbf{r})]$ is a universal functional, since it does not depend on an external potential.

In principle, Theorem 2 gives a method for finding the ground state energy; just try all possible electron densities, and choose the one that gives the lowest energy. This would be such a time-demanding task that it is impossible in practice. In 1965 Kohn and Sham came up with a better method on how to produce a functional $F[n(\mathbf{r})]$ that can produce the ground state energy [30].

2.5.2 The Kohn-Sham ansatz

The problem with the energy expression in Eq. (2.12), is that we do not know the functional $F[n(\mathbf{r})]$. Hohenberg and Kohn only implied that there exists such a functional, and did not clearify its form nor how it is to be constructed. The Kohn-Sham ansatz helps finding this functional and includes a procedure for how to solve the SE [30]. The main idea is to use a system of non-interacting particles with the same ground state density $n(\mathbf{r})$ as the real system. They came up with this form for the functional F[n(**r**)]:

$$F[n(\mathbf{r})] = T[n(\mathbf{r})] + V_{\text{int}}[n(\mathbf{r})] = T_{\text{S}}[n(\mathbf{r})] + E_{\text{H}}[n(\mathbf{r})] + E_{\text{XC}}[n(\mathbf{r})]. \tag{2.13}$$

Here the kinetic energy $T[n(\mathbf{r})]$ is split into two parts; the kinetic energy $T_{\text{S}}[n(\mathbf{r})]$ for the hypothetical non-interacting electrons with the same density as the real system, and a part due to electron correlation that is included in $E_{\text{XC}}[n(\mathbf{r})]$. $E_{\text{H}}[n(\mathbf{r})]$ is the Hartree energy, the energy due to electron-electron Coulombic energy and $E_{\text{XC}}[n(\mathbf{r})]$ is the energy from exchange and correlation. Only the second term is easily expressed, the two others are more complicated. $T_{\text{S}}[n(\mathbf{r})]$ is possible to obtain numerical if we know the wavefunction of the noninteracting system. $E_{\text{XC}}[n(\mathbf{r})]$ is the most difficult part, so let us have closer look at it.

2.5.2.1 The exchange-correlation energy

The functional $E_{\text{XC}}[n(\mathbf{r})]$ is defined as the difference between the true functional $F[n(\mathbf{r})]$ and the remaining terms in Eq. 2.13. In other words; the energy difference between the true total energy of the system and the energy of the auxiliary non-interacting system introduced in the Kohn Sham anzats. $E_{\text{XC}}[n(\mathbf{r})]$ contains all many-particle effects such as the many-particle contribution to the kinetic energy and the effect due to the Pauli exclusion principle and antisymmetrization.

This way $F[n(\mathbf{r})]$ is divided into a known and an unknown part. The exchange correlation functional can further be divided into two parts, the exchange energy $\mathrm{E}_X[\mathrm{n}(\mathbf{r})]$ and the correlation energy $E_\mathrm{C}[n(\mathbf{r})]$; $E_\mathrm{XC}[n(\mathbf{r})] = E_\mathrm{X}[n(\mathbf{r})] + E_\mathrm{C}[n(\mathbf{r})]$

The exchange interaction makes electrons of same spin avoid each other, and is therefore a negative contribution to the total energy. In HF theory this part is included in the Slater determinant by construction, but this is not so in DFT.

The correlation energy is the energy difference between the true ground state of a system, and the energy obtained using the Slater determinant in Hartree-Fock method discussed in section 2.4. The HF method treated the electrons as independent, but electrons are correlated, and since they have the same, negative charge, they tend to avoid each other.

2.5.3 Kohn-Sham equations

Kohn and Sham [30] introduced a set of self-consistent equations that includes the exchange and correlation effects. The main goal with these equations is to solve the many-particle Shcrödinger equation (2.2, 2.4). The basic idea is to reintroduce single particle orbitals into the formalism to treat the kinetic energy using noninteracting pseudo-particles. First, we find an expression for the chemical potential, μ, using 2.13 as the functional $F[n(\mathbf{r})]$ in Eq. (2.12):

$$\mu = \frac{\delta E[n(\mathbf{r})]}{\delta n(\mathbf{r})} = 0 = \frac{\delta T_\mathrm{S}[n(\mathbf{r})]}{\delta n(\mathbf{r})} + \frac{\delta E_\mathrm{H}[n(\mathbf{r})]}{\delta n(\mathbf{r})} + \frac{\delta E_\mathrm{XC}[n(\mathbf{r})]}{\delta n(\mathbf{r})} + \frac{\delta U_\mathrm{ext}[n(\mathbf{r})]}{\delta n(\mathbf{r})} \tag{2.14}$$

$$= \frac{\delta T_\mathrm{S}[n(\mathbf{r})]}{\delta n(\mathbf{r})} + V_\mathrm{H}(\mathbf{r}) + V_\mathrm{XC}(\mathbf{r}) + V_\mathrm{ext}(\mathbf{r}). \tag{2.15}$$

We then introduce a system of noninteracting particles moving in an effective external potential, V_eff. This pseudo-system has the same electron density $n(\mathbf{r})$ as the original system. The energy functional for this system can be expressed as

$$E[n(\mathbf{r})] = T_\mathrm{S}[n(\mathbf{r})] + \int d^3r V_\mathrm{eff}(\mathbf{r}) n(\mathbf{r}), \tag{2.16}$$

which gives the chemical potential

$$\mu = \frac{\delta E[n(\mathbf{r})]}{\delta n(\mathbf{r})} = \frac{\delta T_\mathrm{S}[n(\mathbf{r})]}{\delta n(\mathbf{r})} + V_\mathrm{eff}. \tag{2.17}$$

Since the two systems have the same electron density, they have the same ground state energy if they move in the same effective potential. Combining this equation with Eq. (2.15) gives an expression for this effective potential:

$$V_{\text{eff}}(\mathbf{r}) = V_{\text{H}}(\mathbf{r}) + V_{\text{XC}}(\mathbf{r}) + V_{\text{ext}}(\mathbf{r}). \tag{2.18}$$

This potential can be thought of as the effective external potential in which the noninteracting particles are moving. This system will then give the correct ground state energy. Using this potential in the Shcrödinger equation, we get the Kohn-Sham equations:

$$H_{\text{eff}}(\mathbf{r})\psi_{\text{i}}(\mathbf{r}) = \left[-\frac{1}{2}\nabla^2 + V_{\text{eff}}(\mathbf{r})\right]\psi_{\text{i}}(\mathbf{r}) = \epsilon_{\text{i}}\psi_{\text{i}}(\mathbf{r}) \tag{2.19}$$

The solutions to this SE are called the Kohn-Sham eigenvalues and orbitals, and the ground state electron density is given by the N lowest eigenstates:

$$n(\mathbf{r}) = \sum_{\text{i}=1}^{N} |\psi_{\text{i}}(\mathbf{r})|^2. \tag{2.20}$$

We now have the solution to the ground state problem, but there still remains two problems. The first is; we do not know the exchange correlation functional $V_{\text{XC}}(\mathbf{r})$. The second problem is that $n(\mathbf{r})$ is given by the solution of Eq. (2.19) which depends on $n(\mathbf{r})$. Let us first look at the first problem.

2.5.4 Approximations for the exchange correlation functional

To find the ground state energy, we have to solve the Kohn-Sham equations (Eq. 2.19), i.e. to minimize an energy functional and self-consistently find the solutions to single-particle equations. To be able to do this, we have to specify the exchange-correlation functional. The real form of this functional is unfortunately not known. This means that approximations must be made. We do, however, have to be cautious; an approximated exchange-correlation functional will no longer guarantee that we get the exact ground state energy.

Many classes of exchange correlation functionals have been developed with different approaches, fitting for different purposes. We will take a closer look at three of these. The local density approximation and the generalized gradient approximation, which both are pure DFT functionals, and hybrid functionals which adds a part exact exchange from HF theory.

2.5.4.1 Local Density Approximation (LDA)

For one case, the exchange energy can be derived exactly, and the correlation energy numerically; the uniform electron gas [29, p. 14-15, 215-220]. For this case, the electron density is constant in all space. The easiest approximation to the exchange correlation functional uses this case to construct a Kohn-Sham exchange correlation functional. If we assume that the exchange correlation functional at each point is the exchange correlation functional for the uniform electron gas given the electron density at that point, we get

$$V_{\mathrm{XC}}^{\mathrm{LDA}}(\mathbf{r}) = V_{\mathrm{XC}}^{\mathrm{gas}}[n(\mathbf{r})]. \tag{2.21}$$

This is the Local Density Approximation (LDA), since it only uses the local density to construct an exchange correlation functional. The LDA fits well with bulk materials where the electron density is slowly varying. The electron density for atoms and molecules does not have this property, which means that the LDA is not the best choice for predicting properties in these cases.

2.5.4.2 Generalized Gradient Approximation (GGA)

A second class of exchange correlation functionals also uses the local electron density as in LDA, but this class also includes the local gradient in the electron gas [29, p. 14-15, 215-220]. This is done because real electron densities are not uniform, so by including information about the spatial variation the functional can be improved. This approximation is called the Generalized Gradient Approximation (GGA):

$$V_{\mathrm{XC}}^{\mathrm{GGA}}(\mathbf{r}) = V_{\mathrm{XC}}[n(\mathbf{r}), \nabla n(\mathbf{r})]. \tag{2.22}$$

BLYP is an example of a GGA exchange correlation functional, and it combines the Becke gradient-exchange correction with the Lee-Yang-Parr correlation functional [23]. Although the GGA includes more properties than the LDA, it does not always give better results. But it generally does so for small molecules and atoms.

2.5.4.3 Hybrid functionals

The Kohn-Sham exchange-correlation functional includes the exchange and the correlation effects, which both are unknown. Hartree-Fock theory however, has an exact expression for the exchange energy. Thus, many attempts in coupling HF theory and DFT have been done, and in 1992 Becke [31] was the first that succeeded. Since then, many mixed functionals have been developed. All functionals that mix a part of the nonlocal HF exact exchange with a DFT exchange-correlation functional are called hybrid functionals.

The most popular hybrid functional is the B3LYP functional [29, p. 215-220]. The B3LYP functional can be written as

$$\begin{aligned} V_{\mathrm{XC}}^{B3LYP} =& V_{\mathrm{XC}}^{\mathrm{LDA}} + \alpha_1(E_{\mathrm{X}}^{\mathrm{HF}} - V_{\mathrm{X}}^{\mathrm{LDA}}) + \alpha_2(V_{\mathrm{X}}^{\mathrm{GGA}} - V_{\mathrm{X}}^{\mathrm{LDA}}) \\ &+ \alpha_3(V_{\mathrm{C}}^{\mathrm{GGA}} - V_{\mathrm{C}}^{\mathrm{LDA}}) \end{aligned} \tag{2.23}$$

where $V_{\mathrm{X}}^{\mathrm{GGA}}$ is the Becke 88 exchange functional and $V_{\mathrm{C}}^{\mathrm{GGA}}$ is the Lee-Yang-Parr correlation functional, the same functionals that together make up the BLYP functional mentioned above. $E_{\mathrm{X}}^{\mathrm{HF}}$ is the HF exact exchange, and α_1, α_2 and α_3 are numerical parameters. As we can see, the B3LYP functional combines exchange and correlation functionals from both LDA and GGA with the exact exchange from HF. An other exchange correlation functional is the BHandHLYP functional, which mixes the Lee-Yang-Parr correlation functional with half and half of the Becke exchange functional and the HF exact exchange.

The B3LYP functional, together with some other hybrid functionals, has been highly successful in predicting properties of small molecules. A big advantage with DFT, is that it has low computational costs. However, when HF exact exchange is added, the computational cost is greatly increased.

2.5.5 Solving the Kohn-Sham equation

The second problem is that the Kohn-Sham equations (2.19) have an iterative solution; they have to be solved self-consistently. Kohn and Sham [30] suggested this iterative method to find the ground state energy:

1. Define an initial, starting electron density, $n_0(\mathbf{r})$.

2. Use this electron density to construct $V_{\text{eff}}(\mathbf{r})$ from Eq. (2.18). That is; calculate $V_{\text{XC}}(\mathbf{r})$, $V_{\text{ext}}(\mathbf{r})$ and $V_{\text{H}}(\mathbf{r})$.

3. Calculate a new electron density, $n(\mathbf{r})$, using Eq. (2.19) and Eq. (2.20).

4. Check for self consistency: compare the new ($n(\mathbf{r})$) and the old ($n_0(\mathbf{r})$) electron density. If they are equal with a given accuracy, this is the ground state density, and it can be used to calculate the final energy. If not, return to step 2. The convergence criteria are given as a user input, and are often given as energy changes or changes in bond length or angles.

Chapter 3

Computational methods

3.1 Amsterdam Density Functional (ADF)

The program used in all calculations in this thesis is Amsterdam Density Functional (ADF2009). ADF is a Fortran-based program made to do calculations on atoms and molecules in both gas and liquid phase [32]. The program is based on the Kohn-Sham approach to DFT described in chapter 2, and has been developed since the 1970s. This sections aim is to give a brief introduction to this program and the functions it provides, together with the settings used in this study.

3.1.1 Basis set and atomic coordinates

ADF provides three different coordinate choices; cartesian, internal (Z-matrix) and delocalized coordinates. In all calculations done in this thesis, internal coordinates have been used. The N atoms in the molecule are then named from 1 to N in order of appearance in the input file. The coordinates of the atoms are specified by bond lengths, bond angles, and dihedral angles. For internal coordinates the geometry of the molecule is given by $3N - 6$ coordinates, while the number of coordinates needed for cartesian coordinates are $3N$.

ADF uses Slater Type Orbitals (STOs) as basis functions, in contrast to the Gaussian-type orbitals (GTOs) often used [33]. The advantage of STOs is that it allows the construction of high-quality basis sets with three times less functions

than GTOs with the same basis set quality. A basis set can be characterized by its size and by the level of frozen core approximation [32]. Some of the basis sets available with ADF are these: SZ, DZ, DZP, TZP, and TZ2P, with increasing size and quality. SZ is a single-zeta basis set and DZ is a double one. DZP is in addition polarized, as is TZP but with a core double zeta, valence triple zeta. Finally TZ2P is a core double zeta, valence triple zeta, doubly polarized basis set. In addition there exist special basis sets. The basis set chosen for all computations done below is the TZ2P basis set.

The integration accuracy has been chosen to 6 for all calculations. This accuracy determine the precision for the numerical integrals evaluated during the calculations, and is a number between 0,5 (very inaccurate) and 12 (very accurate) [33]. The precision for the numerical integration is thus calculated in such a way that the user input gives the number of significant digits for the final output [32].

3.1.2 Frozen core

For all GGA-BLYP calculations a small frozen core has been chosen. A frozen core implies that the innermost atomic shells are kept frozen, and this speeds up the computations [32]. For the atom types used here this implies that the 1s orbital will be frozen for oxygen and carbon, and there will be no frozen core for hydrogen. Frozen core is not included for the hybrid functionals in ADF.

3.1.3 Exchange-correlation functionals

The exchange-correlation functional we have used the most is the Generalized Gradient Approximation (GGA) BLYP. This option combines the Becke exchange part with the Lee-Yang-Parr correlation part [32]. The hybrid functionals B3LYP and BHandHLYP have also been used to some extent. These functionals are a combination of the standard GGA with a part Hartree Fock exchange. The B3LYP functional uses 20 % Hartree Fock exchange, while BHandHLYP uses 50 % Hartree Fock exchange.

B3LYP has been chosen because it is one of the most frequently used DFT exchange correlation functionals [19]. One of the disadvantage for this functional, is that since it includes a part exact Hartree Fock exchange, the computational costs are higher than with a pure DFT functional. The main problem, however, is that

B3LYP does not support frequency calculations in ADF. It is thus not possible to validate energy minima and maxima using frequency calculations with B3LYP. BLYP, one of the most popular pure DFT exchange correlation functionals [20], do support frequency calculations in ADF. To be able to find energy minima and maxima, BLYP has therefore been chosen. The third functional, BHandHLYP has been chosen because it consist of even more exact HF exchange than B3LYP, and it is also among the most widely used DFT functionals [21]. (See section 2.5.4 for more details.)

3.1.4 Spin

Generally for the calculations, the spin polarization has been set to zero. This means that the occupation number and the orbitals are identical for spin-α and spin-β molecular orbitals [32]. When a radical is included, the spin polarization has been set to 1, and the spin is set to unrestricted. Then the spin-α and spin-β molecular orbitals have different occupation numbers and spatial orbitals.

3.1.5 Atomic charges

To get insight into the reactivity and bonding of molecules, the atomic charges can be useful. ADF provides three different approaches to calculate the atomic charges; the Hirshfeld scheme, the Voronoi deformation density (VDD) method, and Mulliken population analysis [33]. Here the latter has been chosen to analyze the atomic charges. Population analysis divides the electron density between the nuclei so that every nucleus has a certain number of electrons associated with it [23, p. 79-80]. For Mulliken population analysis, all of the electron density in the orbitals of an atom is allocated to that atom. For overlapping orbitals, the electrons are divided. The charges of the nuclei are then added to get the net charge on the atom.

The different methods available for population analysis give a big variation in the results, and Mulliken population analysis is strongly basis set dependent [23, p. 79-80]. When Mulliken charges are listed in the results, only the charges for some atoms are listed. It has, however, been controlled that the total Mulliken charge for the entire molecule is equal to zero. All charges listed, are calculated with the BLYP functional.

3.1.6 Run types

ADF provides many different run types, i.e. presets for the calculations to be done. The run types used here are geometry optimizations, transition state search, frequency calculations, and old linear transit. Below follows a description of these run types together with the settings applied.

3.1.6.1 Geometry optimization

The geometry optimization is based on a quasi Newton approach [32]. This is done by using an approximate Hessian to compute changes in the geometry to make the gradients vanish. (A Hessian matrix contains second derivatives of the energy.) The Hessian itself is updated during the optimization. When a stationary point on the potential energy surface is found, and this is a minimum point, all the Hessian eigenvalues should be positive. Since internal coordinates have been used, the old branch of optimization method had to be chosen.

The Hessian update scheme was set to auto, and therefore BFGS (Broyden-Fletcher-Goldfarb-Shanno) is used. Convergence criteria were all set to default. This means the criterion for changes in energy is 10^{-3} Hartree, 10^{-3} Hartree/Å for the gradients, 10^{-2} Å for changes in bond lengths, and 0,5 degrees for changes in bond and dihedral angles. The maximum radial and angular step have also been set to default, and that is 0,30 Å and 10 degrees, respectively.

3.1.6.2 Transition state search

A transition state is a saddle point on the potential energy surface. A transition state search is similar to a geometry optimization, but here the Hessian matrix has one negative eigenvalue. To locate a saddle point is much harder than locating a minimum point, mainly because of anharmonicities around it [32].

Most of the settings for geometry optimization also apply to a transition state search, but with some different default values. The default Hessian update scheme used is Powell, the maximum angular step is set to 5 degrees and the maximum radial step is set to 0,20 Å. The reason for more accurate values here is that a better precision is often needed for a transition state search [32]. For a transition state search it is also necessary to specify the mode in which the energy should be maximized. This value is set to 1, so that the mode with the lowest energy is chosen.

3.1.6.3 Frequency calculation

To validate a energy minimum or a transition state, the frequencies and vibration modes need to be calculated. ADF has two choices on how to calculate the frequencies; analytically or numerically. Both methods give the same integration accuracy, but the analytical frequencies can be up to 3-5 times quicker to compute [32]. Here, analytical frequencies are calculated. The calculation of the frequencies uses the solution of the Coupled Perturbed Kohn-Sham (CPKS) equations, which is an iterative process.

Only a limited number of exchange-correlation functionals in ADF supports the calculation of frequencies. One of them is GGA BLYP, but none of the hybrid functionals supports analytical frequency calculations. ADF also provides the Mobile Block Hessian (MBH) method which is useful when calculating vibrational frequencies for a part of a system [32]. In all calculations done below the vibrational frequencies for the entire system have been calculated, and MBH has therefore not been used.

3.1.6.4 Linear transit

A linear transit run is a sequence of constrained geometry optimizations. One chooses an atomic coordinate which are given an initial and a final value. (It is possible to choose more than one coordinate, but we have not done so.) Then the number of steps is specified for the linear change from beginning to end. At each step the atomic coordinates are optimized and the energy calculated, given the locked coordinate. The constrained coordinate is for example a given bond length, an angle, or a dihedral angle. A linear transit run can help finding an exact transition state.

ADF provides two different linear transit run types; the new and the old branch. The one used in the calculations below is the old branch. When the initial and final values for the constrained coordinates are chosen, the number of steps has to be chosen. For a bond length, steps of 0,05 Å have been used. The angular step for a dihedral angle is set to 5 degrees. For example, a 360 degree rotation of a dihedral angle requires 73 steps to move with 5 degree steps all the way round back to the starting position.

3.2 Implementations

For all energy minima calculated with BLYP an unconstrained geometry optimization has been performed, followed by a frequency calculation, to verify that all the frequencies are positive. For all local energy maximum points calculated with BLYP, a transition state search and a frequency calculation were performed. Here all the frequencies were positive, except one, which corresponds to the movement of one or more atoms in the direction of lower energy. For validation of the maximum points, see Appendix C. ADF does not support frequency calculations with B3LYP. This is done for all calculations although not mentioned.

3.2.1 Simplifications of Vitamin E

Vitamin E is a big molecule, at least for doing DFT calculations. All calculations done in this thesis are therefore done on simplifications of vitamin E. In previous studies, different simplifications of vitamin E has been done. Burton and Ingold [9] concluded that it is mainly the two rings that are biologically active when it comes to the antioxidant activity of vitamin E, so all calculations done in this thesis are done on simplifications of vitamin E where the long side chain is removed. This is to avoid high computational costs, and to keep a high performance-to-cost ratio.

In previous studies of vitamin E and vitamin E-like molecules, a range of different simplifications can be seen. The easiest cases are studies done on phenol [34, 35]. Burton and Ingold [9] has done experiments on different phenol antioxidants, and the smallest molecule investigated was 2,3,5,6-tetramethyl-4-methoxyphenon (TMMP) seen in Fig. (3.1a). The larger 2,2,5,7,8-pentamethyl-6-hydroxychroman (PMHC) seen in Fig. (3.1b) was shown to have the same biological reactivity as α-tocopherol in vitro [9]. This molecule is also used in other studies [2, 10, 36].

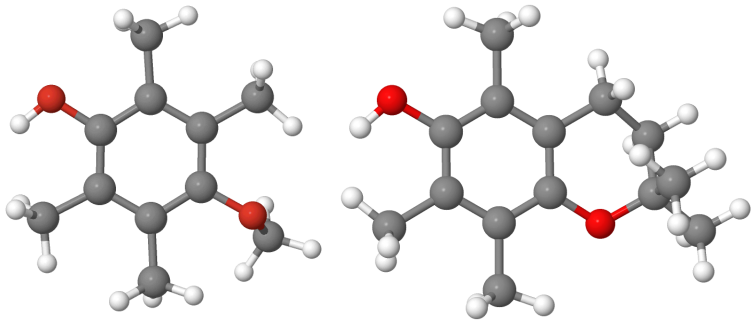

(a) (b)

Figure 3.1: *Two different simplifications of the α-isoform vitamin E. (a) The heterocyclic ring substituted by an oxygen and a methyl group on one side and a methyl group on the other side. (b) The phytyl tail substituted by a methyl group.*

We have chosen two different simplifications of vitamin E in our study, simplification **A** and simplification **B**:

3.2.1.1 Simplification A

The first simplification, hereafter simplification **A**, is almost the same as the molecule Burton and Ingold [9] concluded to have the same biological activity as α-tocopherol. Instead of the two methyl groups on the heterocyclic ring as in Fig. (3.1b), there are two hydrogen atoms. In other words, the long side chain on vitamin E is replaced by a hydrogen atom, and the same goes for the methyl group on the heterocyclic ring. Others have also used this simplification in their study [6, 37]. The α-isoform of simplification **A** can be seen in Fig. 3.2.

3.2.1.2 Simplification B

The easiest simplification, hereafter simplification **B**, consists of only the phenolic ring with the hydroxyl group and none, one, two, or three methyl groups. The heterocyclic ring is in this simplification replaced with two hydrogen atoms. This is a simplification similar to the one used by Burton and Ingold [9], seen in Fig. (3.1a). Although Burton and Ingolds study showed that this molecule only was 9% as reactive as α-tocopherol, a even simpler molecule has been chosen in our study. This is to keep the computational costs down, and to do trial calculations on this small molecule before applying them to simplification **A** with higher com-

putational costs. This way the effect of the heterocyclic ring can be investigated. Others have also used this simplification in their study [37, 34]. The α-isoform of simplification **B** can be seen in Fig. (3.3).

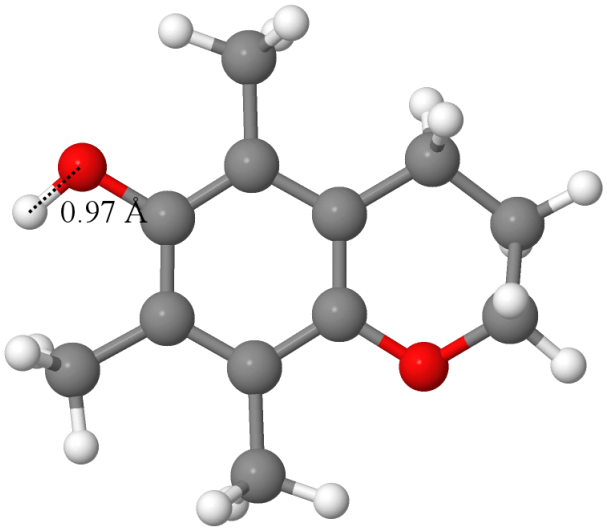

Figure 3.2: *The α-isoform of simplification* **A** *of vitamin E.*

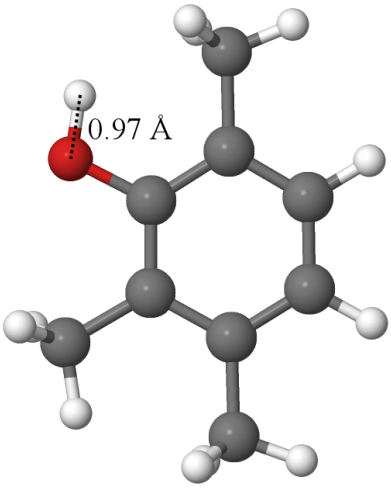

Figure 3.3: *The α-isoform of simplification* **B** *of vitamin E.*

3.2.2 Radicals

To test the antioxidant property of the vitamin E-like molecules, a radical has to be used. The realistic choice would be a lipid, but since this is a large molecule, a simplification has to be done. We have therefore chosen three different radicals for the computations, seen in Fig. (3.4). The simplest is the hydrogen peroxide radical, $^{\bullet}$OOH, seen in Fig. (3.4a), the second is methyl peroxide radical, $^{\bullet}OOCH_3$, seen in Fig. (3.4b), and the largest is ethyl peroxide, $^{\bullet}OOC_2H_5$, seen in Fig. (3.4c). This is the active part of a lipid when it comes to the antioxidant activity of vitamin E. $^{\bullet}OOCH_3$ is the same radical used for a hydrogen transfer in [36], and $^{\bullet}$OOH is the same as used in [34].

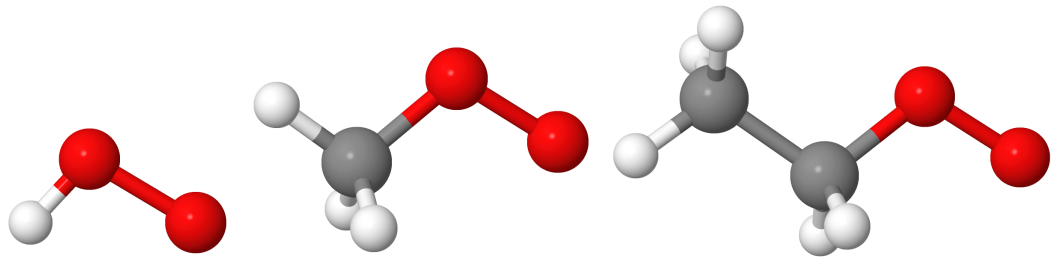

(a) (b) (c)

Figure 3.4: *The three different radicals used in this study; (a) hydrogen peroxide radical, $^{\bullet}OOH$, (b) methyl peroxide radical, $^{\bullet}OOCH_3$, and (c) ethyl peroxide radical, $^{\bullet}OOC_2H_5$.*

3.2.3 Hydrogen transfers

In section 1.1.2, we described the antioxidant properties of vitamin E. When vitamin E breaks the oxidation chain, it donates a hydrogen to a radical. We have studied this reaction with a hydrogen transfer from a vitamin E-like molecule (simplification **A** or **B**) to a radical. A schematic sketch of the energy levels in a hydrogen transfer can be seen in Fig. (3.5).

First the antioxidant, AH, and the radical, R$^{\bullet}$, form a hydrogen bond. Then the hydrogen atom is transferred to the radical. For this to happen, an energy barrier must be overcome. This energy barrier is also called the activation energy for the hydrogen transfer, and is given by $E_a = E(TS) - E(R)$, the energy difference between the transition state and the reactants [36]. After the hydrogen transfer, the complex has a lower energy than prior, and this energy difference is called

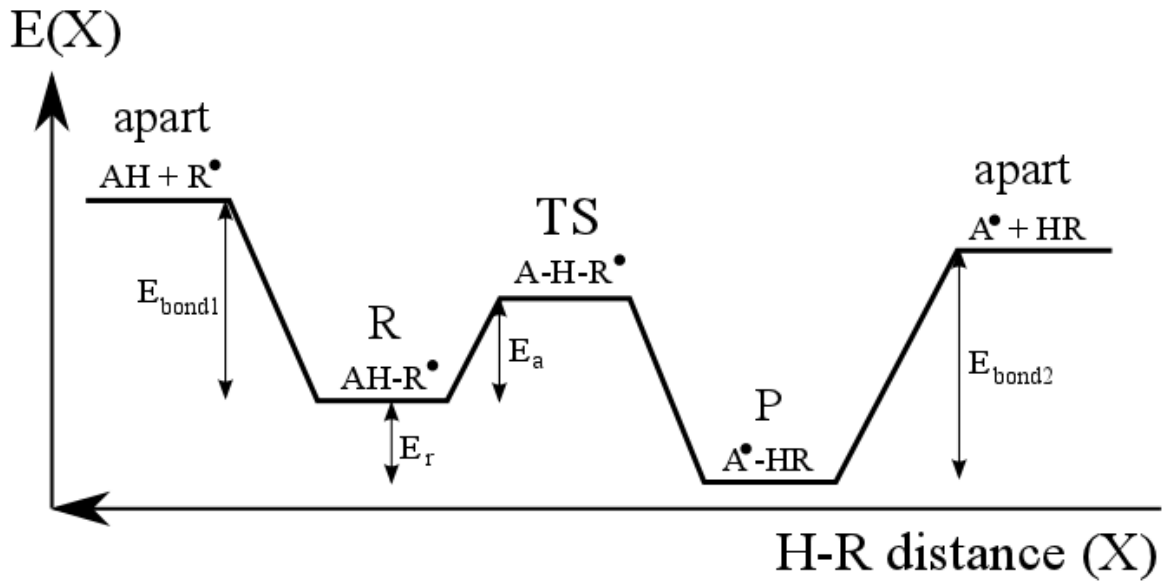

Figure 3.5: *A schematic sketch of the energy levels for a hydrogen transfer between an antioxidant AH and a radical R• as a function of the distance between the radical and the hydrogen atom, X.*

the reaction energy, and is given by $E_\mathrm{r} = E(R) - E(P)$, the energy difference between the products and the reactants [36]. Finally the products have to break the hydrogen bond, creating a radical out of the initial antioxidant and a reduced HR molecule. Our main focus in this study, is the activation energy, but the reaction energy will also be considered.

3.2.4 Comparison of different exchange correlation functionals

Different studies show that especially the BLYP functional underestimates the hydrogen transfer barrier heights [20, 21]. Since we use this functional, a test of its reliability for describing hydrogen transfer reactions has been performed on a simpler system than vitamin E. The reason for choosing a simpler test system, is to save computational costs, and to get a indication of the difference between the functionals before doing hydrogen transfer calculations on the main system.

The test system consists of the simplest radical used in this study, a hydrogen peroxide radical ($^{\bullet}$OOH), with a hydrogen bond to hydrogen peroxide (HOOH), as seen in Fig. (3.6). The hydrogen atom on HOOH bonded to $^{\bullet}$OOH was then transferred to $^{\bullet}$OOH with a linear transit run. The constrained coordinates was the distance between the hydrogen that was being transferred, and the oxygen it is hydrogen bonded to in the radical. This distanced was decreased from 2.00 Å to 0.90 Å. This was done with three different functionals; the GGA functional BLYP and the hybrid functionals B3LYP and BHandHLYP.

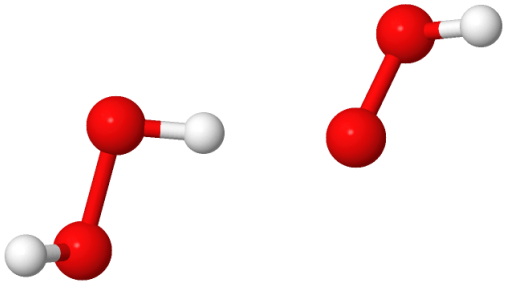

Figure 3.6: *HOOH with a hydrogen bond to* $^{\bullet}$*OOH*

3.2.5 Rotation of the hydroxyl group on different isoforms

The hydroxyl group on vitamin E can rotate out of the plane of the phenolic ring and out of equilibrium. This creates an exited state for the molecule, and changes the electron distribution [18]. We have studied the activation energy for the rotation of this group to see how this rotation affects the energy of the molecule.

A controlled rotation of the hydroxyl group has been done with a linear transit run. This has been done for both the α-, β-, γ-, and the δ-isoform together with an isoform with no methyl groups at all. The isoform of vitamin E with no methyl groups does not occur naturally, but is considered here to study the effect of the methyl groups. The calculations have been done on both simplifications of vitamin E. Accurate energy minima and maxima have been localized with an unconstrained geometry optimization and transition state search, respectively, with both the BLYP and the B3LYP functionals. A full 360 degree rotation of the dihedral angle has been performed. The C-C-O-H dihedral angle used as reaction coordinate is shown in Fig. (3.7).

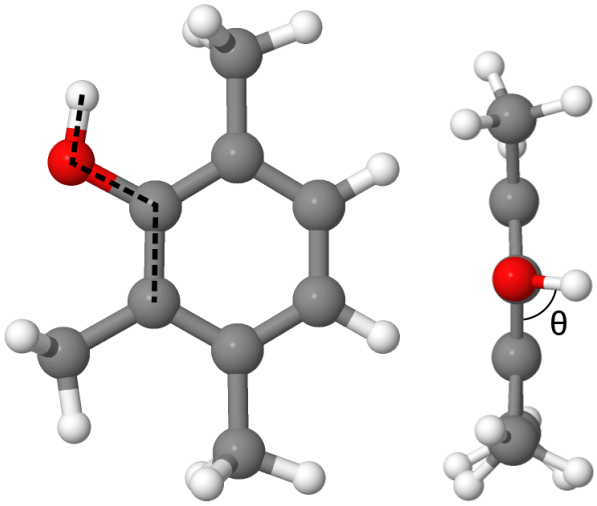

(a) (b)

Figure 3.7: *The dihedral angle reaction coordinate. (a) The four atoms that make up the dihedral angle (here 180 degrees). (b) The molecule viewed along the C-O rotation axis.*

3.2.6 Rotation of hydroxyl group hydrogen bonded to different radicals

We have also done calculations on the rotation of the hydroxyl group where the hydroxyl group is hydrogen bonded to a radical, $^{\bullet}$OOH or $^{\bullet}$OOCH$_3$. The rotation has been done as described in section 3.2.5. These calculations have been done only for simplification **B** with the BLYP functional, and only for the α-isoform. The initial position of the hydroxyl group is at its energy minimum, i.e. in the phenolic plane. It is then rotated out of the plane towards the perpendicular state. Here only a 180 degree rotation of the dihedral angle shown in Fig. (3.7) has been done. Figure (3.8a) and (3.8b) show the initial geometry for the two molecules where the hydroxyl group was rotated.

This was done to see which effect the orientation of the hydroxyl group had when hydrogen bonded to a radical. We also planned to carry out a hydrogen transfer calculation from the transition state of the rotation of the hydroxyl group, but because of problems with convergence, lack of time and the results from the rotation of the hydroxyl group bonded to a radical, this was not done.

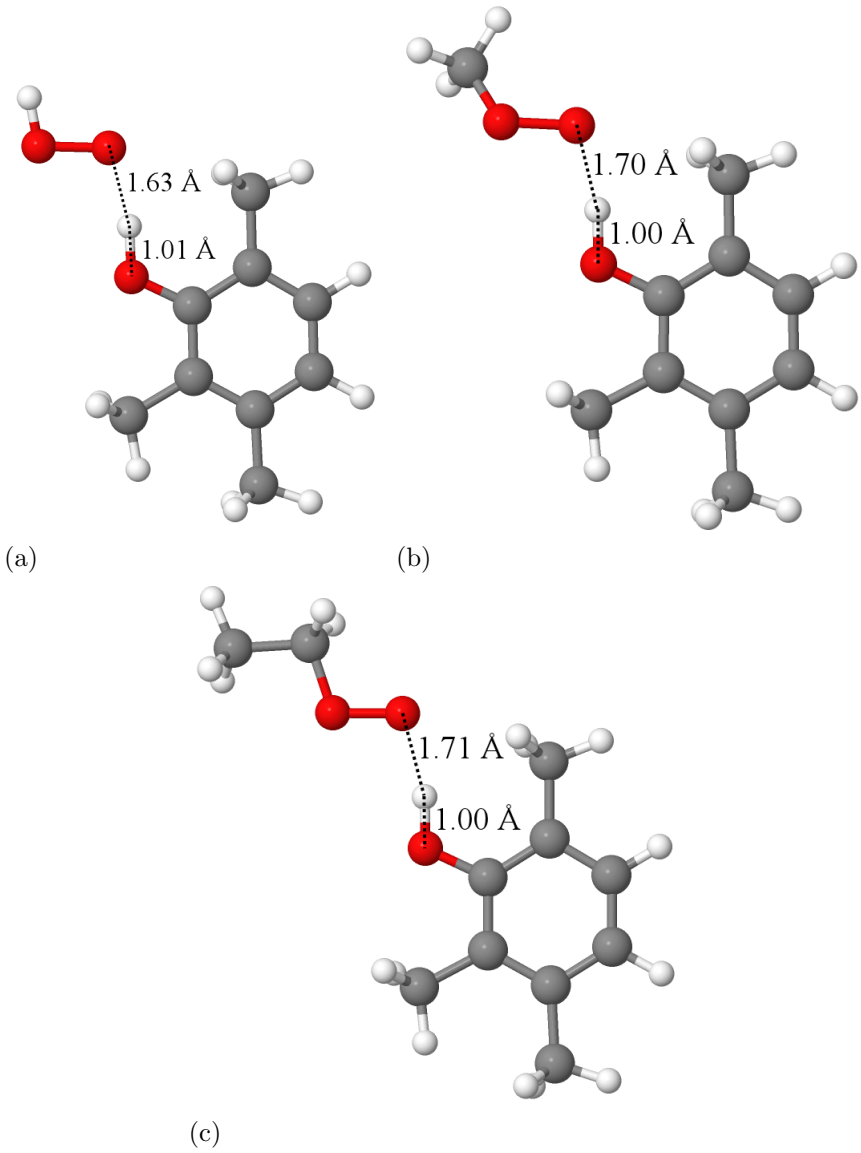

Figure 3.8: *The α-isoform of simplification* **B** *with hydrogen bonds to three different radicals; (a) OOH, (b) $OOCH_3$, and (c) OOC_2H_5.*

3.2.7 Hydrogen transfer from simplification A and B to different radicals

In section 1.1.2 we described the antioxidant properties of vitamin E. One way for vitamin E to break the oxidation chain, is to donates a hydrogen atom to a radical. We have studied this reaction with a hydrogen transfer from a vitamin E-like molecule (simplification **A** or **B**) to a radical. The activation energy, or barrier height, and the reaction energy for the reaction has thus been found. Only the α-isoform, the isoform with three methyl groups are considered here. This isoform is our main focus because it is the most biological active isoform [4, 5, 6], and the one the human body prefers. Thus it is the most interesting isoform to study.

Simplification **B** with a hydrogen bond to three different radicals, $^{\bullet}OOH$, $^{\bullet}OOCH_3$, and $^{\bullet}OOC_2H_5$, can be seen in Fig. (3.8). In Fig. (3.9), simplification **A** can be seen with a hydrogen bond to two different radicals; $^{\bullet}OOCH_3$ and $^{\bullet}OOC_2H_5$. From these stable geometries, hydrogen transfer calculations have been carried out for both simplification **A** and **B**. This has been done with a linear transit calculation using the BLYP functional. The bond length between the hydrogen in the hydroxyl group and the oxygen to which it is bonded in the radical has been gradually decreased from 2,00 Å to 0,90 Å. The systems were given no other constraints than this bond length.

Geometry optimizations for the two energy minima on the energy curve, i. e. before and after the transfer, have also been carried out without any constraints, together with a transition state search. These three calculations have all been done with both the BLYP and the B3LYP functionals.

In reality, vitamin E and the lipid radical are both locked in a biological membrane. Thus we can expect the two molecules to be unable to move as freely relative to each other as is allowed in this hydrogen transfer model. We could of course add more constrained coordinates, and lock the radical and the vitamin E simplification into certain positions relative to each other. An argument in favor of this, is that a hydrogen atom is very small, so the hydrogen transfer will probably happen much faster than the time needed to move the big main molecules.

The main problem with such an approach, is that we do not know which distance would be the most realistic, neither how to arrange the molecules relative to each other. The real location and arrangement of vitamin E is as mentioned in section 1.1 not known [7]. This would make the computations and results more complex and difficult, since we would not be able to know if a realistic arrangement

of the molecules was achieved, and therefore not if a realistic energy barrier was found. We can also assume that the molecules are able to move slightly relative to each other, so to lock their internal positions entirely would neither be a realistic solution. We have therefore selected the constrained coordinates as described above, with the error this may lead to in mind.

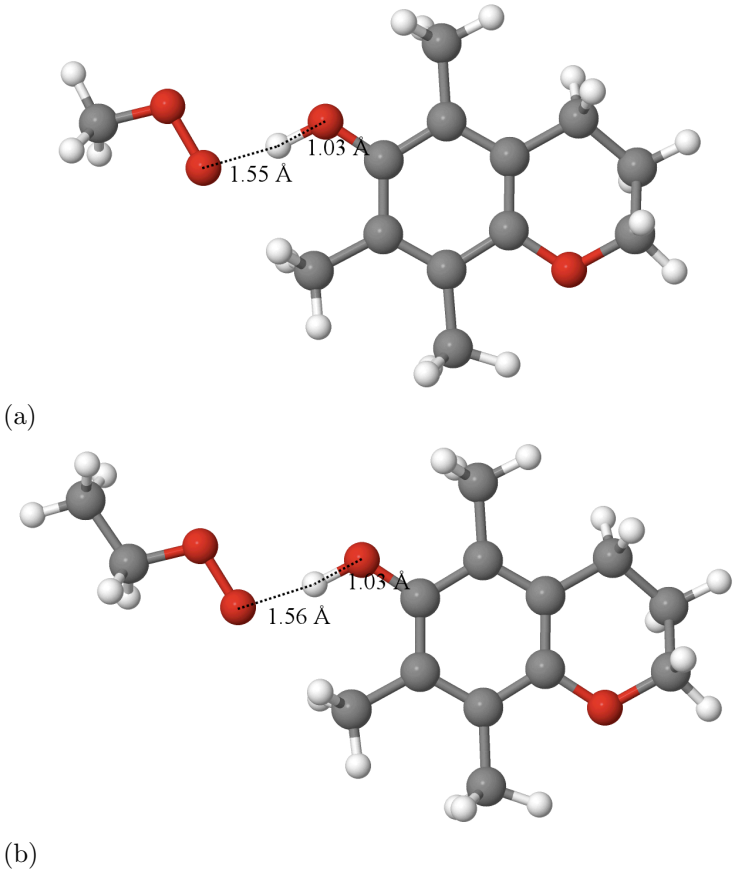

Figure 3.9: *The α-isoform of simplification* **A** *with hydrogen bonds to two different radicals; (a) $OOCH_3$ and (b) OOC_2H_5.*

Chapter 4

Results and discussion

In this section the results of the calculations described in section 3.2 are presented and discussed. First the bonding energies which make the basis for all graphs are presented together with the total energy for every single component. Then the results from the investigation of the reliability of the functional BLYP against the functionals B3LYP and BHandHLYP on the small HOOH-$^{\bullet}$OOH-system follow, before the results from the rotation of the hydroxyl group on the vitamin E simplifications. The simplifications can be seen in Fig. (3.2) for simplification **A** and in Fig. (3.3) for simplification **B**. The results from the hydrogen transfer from the two different simplifications of vitamin E to three different radicals follows next, before the results from the rotation of the hydroxyl group on the vitamin E simplifications hydrogen bonded to different radicals. Finally, the results in general are discussed.

4.1 Bonding Energies

In all calculations, 16 different molecules and complexes of these have been used. These molecules can all be seen in Appendix A. The total energy for all single components, calculated with both the BLYP and B3LYP functional, are presented in Table 4.1. It is observed that the energies calculated with the B3LYP functional are approximately 18-38 % larger than the energies calculated with the BLYP functional. The largest relative difference is for the smallest molecules, while the relative difference decreases with increasing size of the molecule.

Table 4.1: *Total Energy for all molecules that is being used in the calculations. The first column shows the energies calculated with the BLYP functional, and the second shows the energies calculated with the B3LYP functional.*

	Molecule/Radical	BLYP	B3LYP
Radicals	$^{\bullet}$OOH	-12,6877 eV	-17,4470 eV
	HOOH	-17,4515 eV	-22,7809 eV
	$^{\bullet}OOCH_3$	-28,3847 eV	-35,8420 eV
	$HOOCH_3$	-33,0356 eV	-41,0809 eV
	$^{\bullet}OOC_2H_5$	-44,2622 eV	-54,4735 eV
	$HOOC_2H_5$	-48,8928 eV	-59,6948 eV
Simplification **B**	No methyl	-78,6284 eV	-93,6104 eV
	δ	-94,4389 eV	-112,1778 eV
	γ	-110,1820 eV	-130,6556 eV
	β	-110,2471 eV	-130,7290 eV
	α-radical	-121,4415 eV	-144,0304 eV
	α	-135,9714 eV	-149,1863 eV
Simplification **A**	No methyl	-124,4176 eV	-148,7217 eV
	δ	-140,2248 eV	-167,2109 eV
	α-radical	-167,3850 eV	-199,2648 eV
	α	-171,6186 eV	-204,1556 eV

As described in section 3.2.7, hydrogen transfer computations have been run for both simplification **A** and **B** to three different radicals. Table 4.2 shows the energies before and after this hydrogen transfer between simplification **B** and a hydroperoxide radical; $^{\bullet}$OOH, $^{\bullet}OOCH_3$, or $^{\bullet}OOC_2H_5$. The total energy for the components apart is the sum of the single component energies from Table 4.1. The energy for the vitamin E simplification with a hydrogen bond to a radical can also be seen, and the difference between these two energies are the bonding energies.

A trend for all results in Table 4.2 is that the bonding energies decreases with increasing size of the hydroperocide. This means that the hydrogen bond gets weaker, and the complex less stable for a big radical than for a small. It can also be noticed that the energy for the hydrogen bonded system is more negative after the hydrogen transfer than before, which implies that the system is more stable after the hydrogen transfer. We will discuss this in more detail later.

Table 4.2: *Bonding energies for simplification* **B** *bonded to three different radicals using the BLYP functional. The first column shows the total energy of the separated parts. The second column shows the energy of the molecules bonded together with a hydrogen bond between the hydrogen atom on the OH group on the vitamin E simplification and the oxygen on the radical. The third column shows the energy of the hydrogen bond made between simplification* **B** *and the radical.*

Radical	Energy apart	Energy bonded	Bonding energy
$^{\bullet}$OOH	-138,6604 eV	-138,9242 eV	0,2638 eV
After transfer	-138,8930 eV	-139,1876 eV	0,2946 eV
$^{\bullet}OOCH_3$	-154,3574 eV	-154,5897 eV	0,2323 eV
After transfer	-154,4771 eV	-154,7472 eV	0,2701 eV
$^{\bullet}OOC_2H_5$	-170,2349 eV	-170,4610 eV	0,2274 eV
After transfer	-170,3343 eV	-170,5338 eV	0,1995 eV

Table 4.3: *Bonding energies for simplification* **A** *bonded to two different hydroperoxide radicals,* $^{\bullet}OOCH_3$ *and* $^{\bullet}OOC_2H_5$*, using the BLYP functional. The first column shows the total energy of the separated parts.The second column shows the energy of the molecules bonded together with a hydrogen bond between the hydrogen atom on the OH group on the vitamin E simplification and the oxygen on the radical. The third column shows the energy of the hydrogen bond made between simplification* **A** *and the radical.*

Radical	Energy apart	Energy bonded	Bonding energy
$^{\bullet}OOCH_3$	-200,0033 eV	-200,3194 eV	0,3161 eV
After transfer	-200,4206 eV	-200,6999 eV	0,2793 eV
$^{\bullet}OOC_2H_5$	-215,8808 eV	-216,1776 eV	0,2968 eV
After transfer	-216,2778 eV	-	-

Table 4.3 shows the same energies as Table 4.2, but for simplification **A** instead of simplification **B**. Only results with the two largest radicals, $^{\bullet}OOCH_3$ and $^{\bullet}OOC_2H_5$, can be found here. The state with simplification **A** hydrogen bonded to $^{\bullet}$OOH was found to be unstable. When a geometry optimization was run for this complex, the hydrogen atom on the hydroxyl group spontaneously broke its bond with simplification **A** and made a bond with $^{\bullet}$OOH, a hydrogen transfer. $HOOC_2H_5$ hydrogen bonded to the simplification **A** radical did not converge, and results from this state can thus not be seen in Table 4.3.

The same trends as in Table 4.2 can be seen in Table 4.3, with a decreasing bonding energy with an increasing size of the hydroperocide. By comparison of the bonding energies for the two simplifications, we can see that the bonding energies for simplification **A** are observed to be larger than those for simplification **B**. This indicates that simplification **A** makes stronger hydrogen bonds to the radicals than simplification **B**.

In all graphs following below, the zero point energy has been chosen to be the total energy of the components apart before the hydrogen transfer, i.e. the energies before the hydrogen transfer in the first column in Table 4.2 and 4.3.

4.2 Comparison of different exchange correlation functionals

In section 3.2.4, we described a test to investigate the energy barrier heights produced by different exchange-correlation functionals in a hydrogen transfer reaction. The system whom the test was run on, can be seen in Fig. (4.1). Here Fig. (4.1a) shows the stable state before transferring hydrogen from HOOH to $^{\bullet}$OOH, Fig. (4.1b) shows the transition state for the hydrogen transfer, and Fig. (4.1c) shows the final geometry optimized state after the hydrogen transfer. The total energy curve for the hydrogen transfer can be seen in Fig. (4.2) for the three different functionals, BLYP, B3LYP and BHandHLYP.

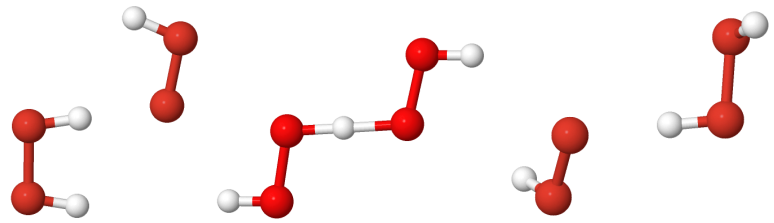

Figure 4.1: *Three states for the hydrogen transfer from HOOH to $^{\bullet}$OOH. (a) Geometry optimized state before the hydrogen transfer, (b) the transition state, and (c) the geometry optimized state after the hydrogen transfer*

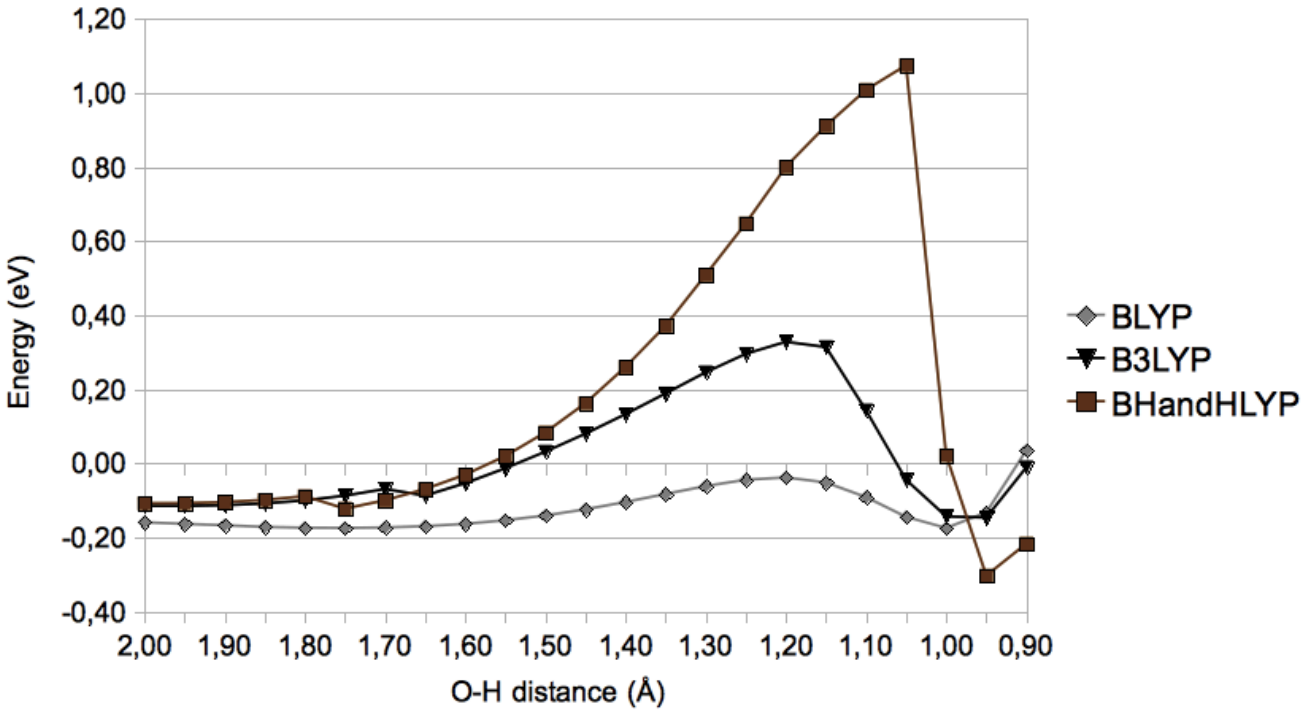

Figure 4.2: *Energy curves for the hydrogen transfer from HOOH to $^{\bullet}$OOH for the three different functionals BLYP, B3LYP, and BHandHLYP. The curves show the energy as a function of the distance between the hydrogen which is transferred and the oxygen atom in $^{\bullet}$OOH.*

As can be seen in Fig. (4.2), the three functionals produces significant different barrier heights. The barrier heights have been calculated as the energy difference between the energy for the transition state search for the maximum point, and the energy from geometry optimization prior to the transfer. This shows that the BLYP functional gives the smallest barrier of 0,136 eV at a H-O bond length of about 1,29 Å, the B3LYP functional gives a barrier of 0,446 eV at a H-O bond length of about 1,18 Å, and the BHandHLYP functional gives the largest barrier of 1,011 eV at a H-O bond length of about 1,18 Å.

As we see from these results, the unrestricted transition states have been shifted to the left as compared with the curves in Fig. (4.2), i.e. towards the HOOH molecule. The barrier heights is also a bit lower than what the graph shows. This is predictive, since a linear transit run forces a certain geometry upon the system. The real transition state is thus not guaranteed to be found with a linear transit run, but it can give an approximate location. It can also be noticed in Fig. 4.2 that

the energy minima before and after the hydrogen transfer has different energies despite the symmetric nature of the calculations. This is due to the different orientation and geometry of the system before and after the reaction.

The results from this hydrogen transfer are consistent with the results found previously, i.e. in [21], where BHandHLYP were found to give the highest energy barrier, and BLYP the smallest. Our study shows a difference where BHandHLYP results in 2,3 times higher energy barrier than B3LYP, and B3LYP results in a energy barrier 3,3 times higher than BLYP. This is a larger difference than the one found in [21], but this study investigated hydrogen atom addition, while our study is hydrogen transfer.

It is not obvious which functional gives the closest value to the actual barrier height, since we do not have any experimental data for comparison. Still, we can assume the barrier height found by BLYP to be too small, since many studies of hydrogen barrier heights with DFT BLYP show that this functional underestimates the barrier heights, i.e. [38]. B3LYP has also often been shown to underestimate the activation energy for hydrogen transfers in many cases [39, 34], but at least we can assume that it provides better results the the BLYP functional. The BLYP and the B3LYP functionals are the ones used in the rest of the calculations.

4.3 Rotation of the hydroxyl group on different isoforms

As we described in section 3.2.5, a rotation of the hydroxyl group on the five isoforms of the vitamin E simplifications has been done. The isoforms can be seen in Fig. (A.2) for simplification **B**, and in Fig. (A.3) for simplification **A** in Appendix A. The results from these calculations can be seen in Fig. (4.3-4.7) and in Table 4.4. Figure (4.3) ans (4.4) shows examples of dihedral angle rotations on the α-isoform of simplification **B** and **A**, respectively. The graphs with the energy curves for the rotation of the C-C-O-H dihedral angle can be seen in Fig. (4.5) for simplification **B** and in Fig. (4.6) for simplification **A**. All graphs are plotted from calculations done with the BLYP functional. In Fig. (4.7) the rotation curves for the rotation of the hydroxyl group on the α-isoform of the two simplifications are shown, since this isoform are the main focus in this study. The energy barriers for the rotation of the hydroxyl group calculated with both the BLYP and the B3LYP functional are listed in Table 4.4.

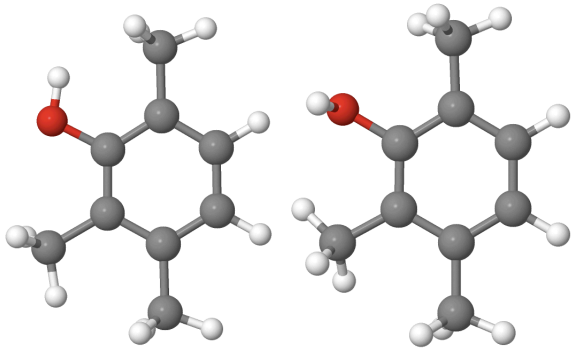

(a) (b)

Figure 4.3: *The α-isoform of simplification* **B**. *(a) The geometry optimized energy minimum for the rotation of the hydroxyl group. (b) The transition state for the rotation of the hydroxyl group.*

The geometry shown in Fig. (4.3a) and (4.4a) correspond to the global minimum for the rotation of the hydroxyl group on simplification **B** and **A**, respectively. For simplification **B**, this is the state which results in the minimum point at 180 degrees in the graph in Fig. (4.5), with the hydrogen atom pointing towards methyl group number one. For simplification **A**, the geometry in Fig. (4.4a) results in the minimum energy at 0 degrees in in the graph in Fig. (4.6), with the hydrogen atom pointing toward methyl group number two. The difference in the global energy minima for the two simplifications can be seen clearer in Fig. (4.7).

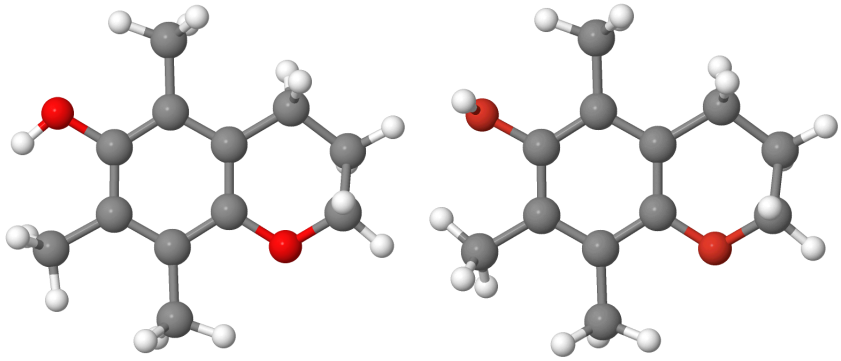

(a) (b)

Figure 4.4: *The α-isoform of simplification* **A**. *(a) The geometry optimized energy minimum for the rotation of the hydroxyl group. (b) The transition state for the rotation of the hydroxyl group.*

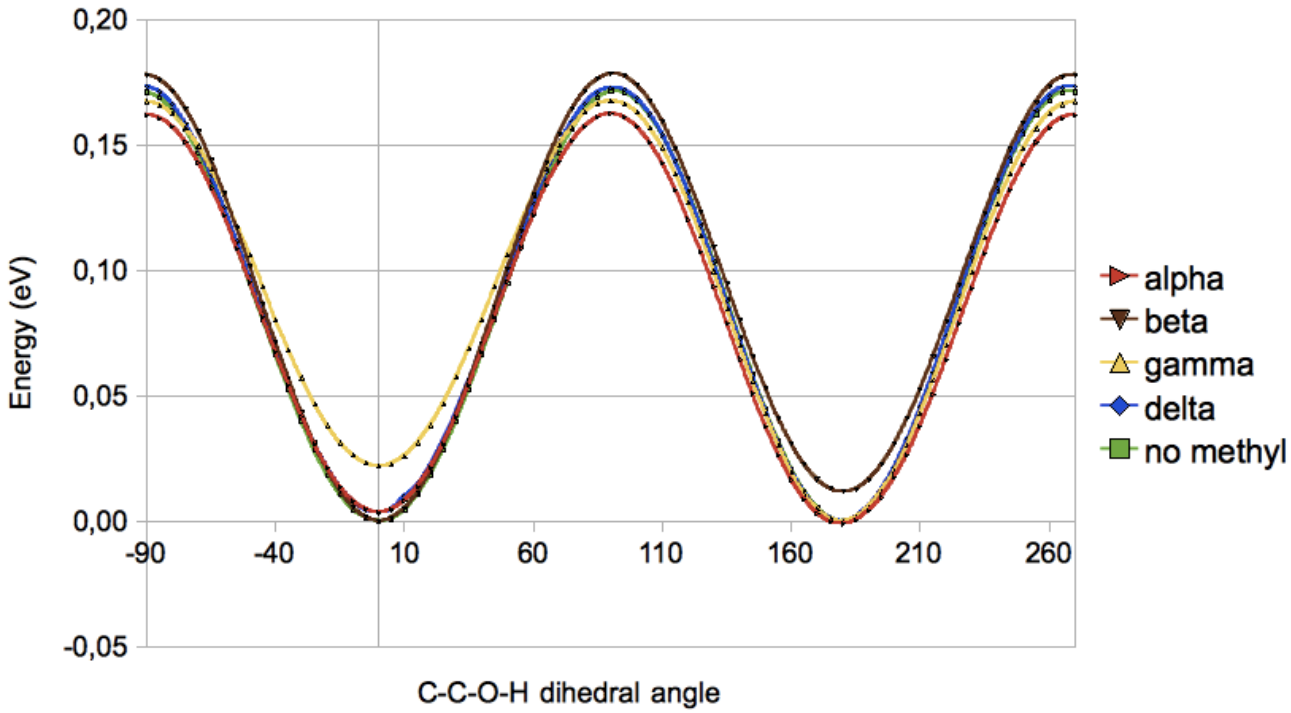

Figure 4.5: *Energy curves for rotation of the OH group on different isoforms of simplification* **B** *of vitamin E calculated with the BLYP functional. The curves show the energy as a function of the C-C-O-H dihedral angle.*

As we see in Fig. (4.5) and (4.6), all isoforms of both simplifications have their local energy minima with the hydroxyl group in the phenolic plane, at 0 and 180 degrees. The transition states are at -90 and 90 degrees, when the hydroxyl group is pointing out of this plane. This agree with [18]. For simplification **A**, the rotational curves for the β and γ-isoform are not shown. This is due to problems with convergence for the rotation of the hydroxyl groups on these isoforms.

As seen in Fig. (4.5), the energy curves for the different isoforms have different levels of symmetry. The isoform with no methyl groups has a totally symmetric energy curve for simplification **B**, and the energy curves for the α and δ-isoforms are also almost symmetric. These are reasonable results, since the isoform of simplification **B** with no methyl groups is totally symmetric. The α and δ-isoforms are also almost symmetric. The α-isoform with its three methyl groups has methyl groups on the nearest carbon atoms on both sides of the hydroxyl group. The δ-isoform with one methyl group has hydrogen atoms on the neighbor carbon atoms around the hydroxyl group. It can however be noticed that the energy minima

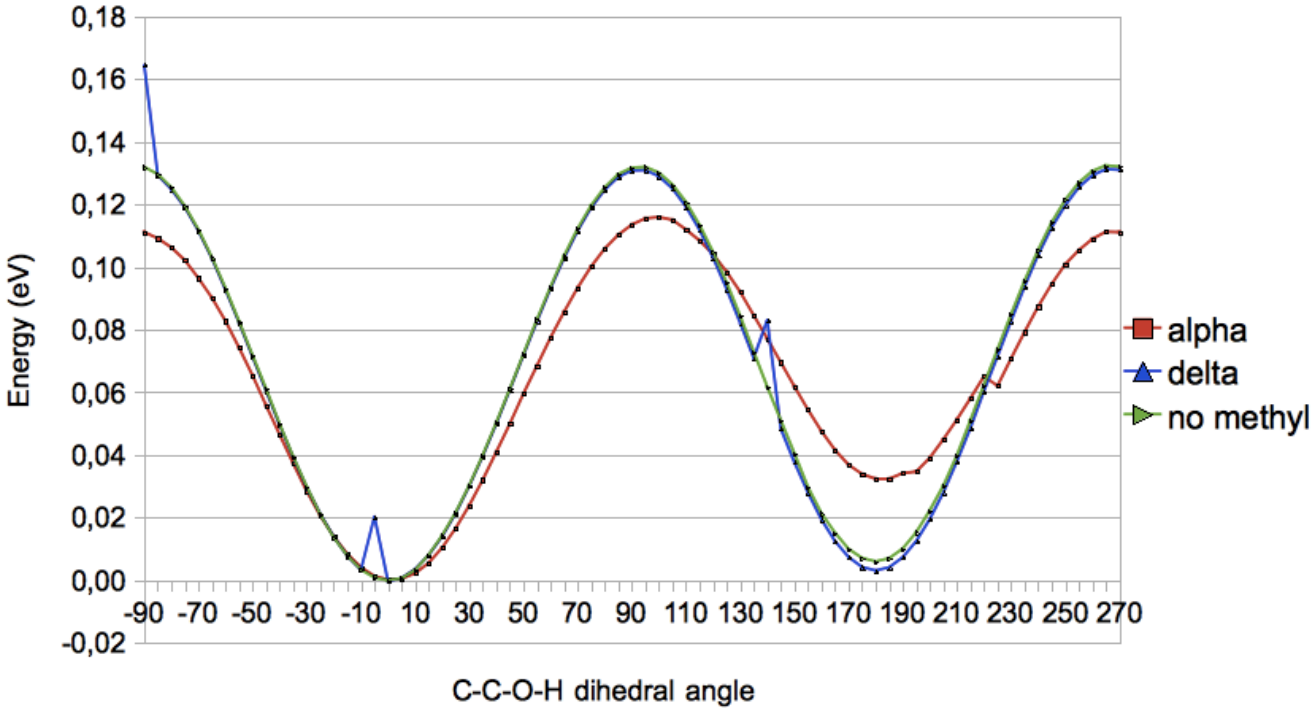

Figure 4.6: *Energy curves for rotation of the OH group on different isoforms of simplification* **A** *of vitamin E calculated with the BLYP functional. The curves show the energy as a function of the C-C-O-H dihedral angle.*

at 180 degrees has a slightly lower energy than the one at 0 degrees for both these isoforms. At 180 degrees, the hydroxyl group points towards the side with one methyl group for the α-isoform, and the side with no methyl groups for the δ-isoform.

The energy curves for the rotation of the hydroxyl group on the β- and γ-isoform of simplification **B** (Fig. 4.5) are, on the other hand, not symmetric. This is also consistent with the geometry of these isoforms. The energy energy curve for the γ-isoform has the lowest level of symmetry. This is also the least symmetric isoform, since it has two methyl groups on the same side. The geometry where the hydroxyl group points towards the other side results in the global energy minimum. The β-isoform also has two methyl groups, but these are placed on different sides of the hydroxyl group. On one side, the methyl group is placed on the carbon atom next to the hydroxyl group, and on the other side it is placed further away. The global energy minima is obtained when the hydroxyl group point towards the side where the methyl group is placed furthest away.

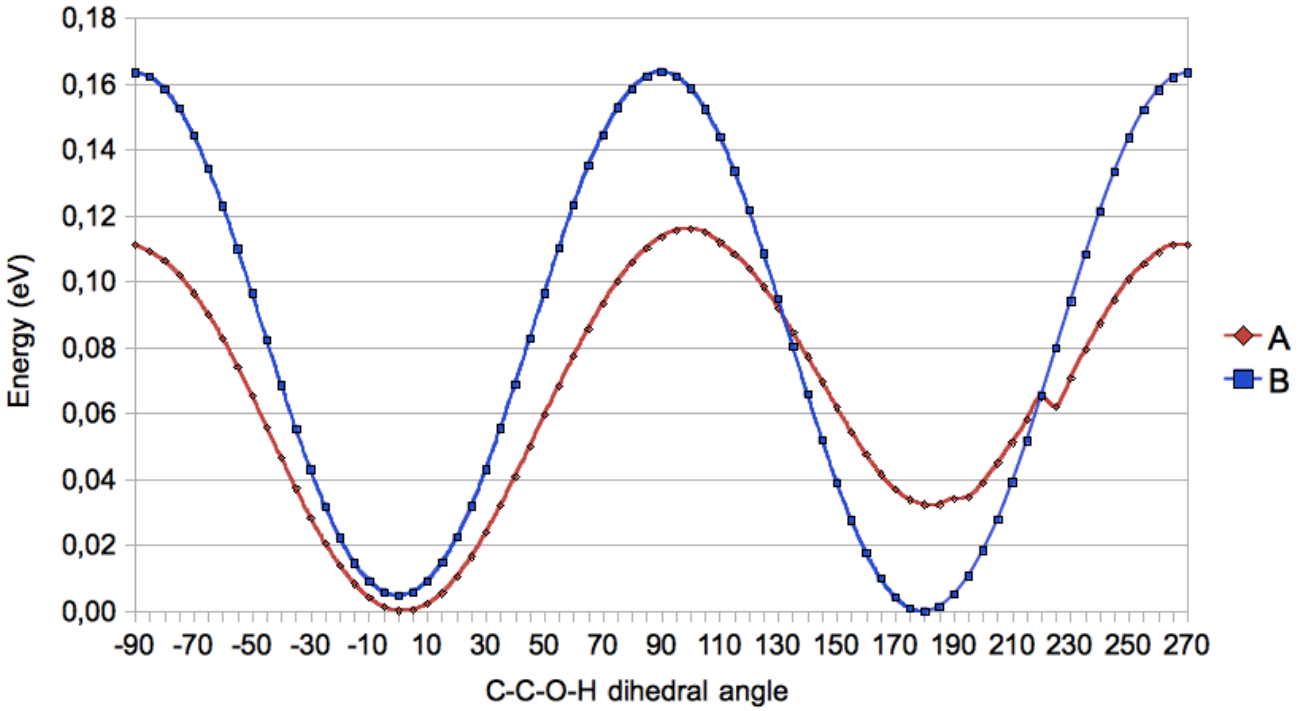

Figure 4.7: *Energy curves for rotation of the OH group on the two different simplifications of the α-isoform of vitamin E calculated with the BLYP functional. The curves show the energy as a function of the C-C-O-H dihedral angle.*

In general, the geometry causing the global minima for all isoforms of simplification **B**, is when the hydroxyl group point towards the side with the fewest methyl groups, or towards the side where the methyl group is furthest away. An explanation of this can be that the methyl group is larger than a single hydrogen atom, and thus the hydrogen atoms on the methyl group comes closer to the hydroxyl group than the hydrogen atom. However, the methyl group is not big enough to cause steric interactions, i.e. repulsion due to the fact that two atoms can not occupy the same amount of space, so the explanation must lay in electrostatic interactions.

The hydrogen atom in the hydroxyl group obtains a positive partial charge, and the single hydrogen atom on the carbon atom next to it obtains a partial negative charge. Thus an attraction between these atoms is expected. On the methyl group, the hydrogen atoms obtains a partial negative charge, and the carbon atom a partial positive charge. The positive charge on the carbon atom is more than twice the size of the negative charge on the hydrogen atoms. Although the

hydrogen atom is positioned closer to the hydrogen atom in the hydroxyl group than the carbon atom, a total repulsion is expected between the methyl group and the hydroxyl group causing an increase in energy. For the α-isoform a bigger repulsion is experienced when the hydroxyl group points towards the side with two methyl groups close to each other. This may be caused by the interaction between the methyl groups.

Simplification **A** provides different energy curves than simplification **B**. For simplification **A**, the energy curve for the isoform with no methyl groups is no longer symmetric, as seen in Fig. (4.6). The curve is far less symmetric for the α- and δ-isoform as well. The geometry causing the global energy minima for all these three isoforms is when the hydroxyl point towards group two as in Fig. (4.4), and away from the heterocyclic ring. The energy curves for the α-isoform of both simplifications can be seen in Fig. (4.7), and here the differences is seen more clearly. The global energy minima is not the same, the energy barriers are different, and the curves have different degree of symmetry. Since the only difference between simplification **A** and **B** is the heterocyclic ring, we expect the explanation to lie here.

For all global energy minima and energy maxima, a geometry optimization and transition state search, respectively, have been run with both the BLYP and the B3LYP functional in order to find the energy barrier for rotation of the hydroxyl group, seen in Table 4.4. As seen above, the different isoforms and simplifications results in different barrier heights for rotation of the hydroxyl group, and so does the functionals. Fig. (4.5) and (4.6) shows that each energy curve has a local and a global energy minimum. The barrier heights in Table 4.4 are computed from the most stable state (the global minimum) to the transition state.

A trend seen in Table 4.4, is that the B3LYP functional produces lower barrier heights than the BLYP functional for all cases. Simplification **B** also give lower energy barriers than simplification **A**. The isoforms with fewest methyl groups give the highest energy barriers, and the barrier height decreases with increasing number of methyl groups. This is the case for both simplifications and both functionals, and indicates that the methyl groups do not lower the transition state energy, but makes the local energy minima less stable. This may give us an indication of why the α-isoform is preferred for uptake in the human body. According to [18], there is a greater chance for a hydrogen transfer instead of other antioxidant action reactions when the hydroxyl group is at its perpendicular state. Since the α-isoform has the lowest barrier for rotation of the hydroxyl group, the probability of being at the perpendicular state increases. This might increase the reactivity. We will

discuss this further later.

Table 4.4: *Rotation barrier for rotation of the hydroxyl group. The values are calculated as the energy difference between the most stable state and the transition state. Results for both simplifications of vitamin E is shown, calculated with both the BLYP and the B3LYP functional.*

Simplification	Functional	no methyl	α	β	γ	δ
B	BLYP	0,1715 eV	0,1623 eV	0,1788 eV [1]	0,1676 eV	0,1729 eV [1]
B	B3LYP	0,1590 eV	0,1362 eV	0,1705 eV	0,1388 eV	0,1572 eV
A	BLYP	0,1352 eV	0,1156 eV	-	-	0,1309 eV
A	B3LYP	0,1222 eV	0,1038 eV	-	-	-

4.4 Hydrogen transfers from vitamin E simplifications to different radicals

As described in section 3.2.7, a hydrogen transfer calculation has been carried out from both simplification **A** and **B** to three different radicals. The results from these computations are presented and discussed below. First for simplification **B**, then for simplification **A**. A comparison of the results obtained with the two simplifications can be found in the next section.

4.4.1 Simplification B

Figure (4.8) shows the energy curves for the hydrogen transfer from simplification **B** to three different radicals; $^{\bullet}OOH$, $^{\bullet}OOCH_3$ and $^{\bullet}OOC_2H_5$, using the BLYP functional. A geometry optimization before the hydrogen transfer and a transition state search have bee run for both the BLYP and the B3LYP functional. The energy barriers have been calculated as the energy difference between these states, and the results can be seen in Table 4.5. The energy differences between the stable states before and after the hydrogen transfer, the reaction energy, can be found in Table 4.6. Table 4.7 shows the Mulliken charges for the three stable states before

[1]The frequency calculation shows one imaginary frequency for the geometry optimization, and one extra for the transition state search. Both corresponding to the rotation of the methyl group furthest away from the hydroxyl group. The maximum energy difference for the rotation of this group is 0,003 eV for the β-isoform, and 0,0015 eV for the δ-isoform. Since no geometry without this imaginary frequency was found, the energies from these calculations are listed here.

the hydrogen transfer. The geometries for the energy minima before the hydrogen transfer can be seen in Fig. (4.9), with the atom names included. Geometries corresponding to every second point on the graph for $^{\bullet}$OOH in Fig. (4.8) can be seen in Fig. (B.1) in appendix B.

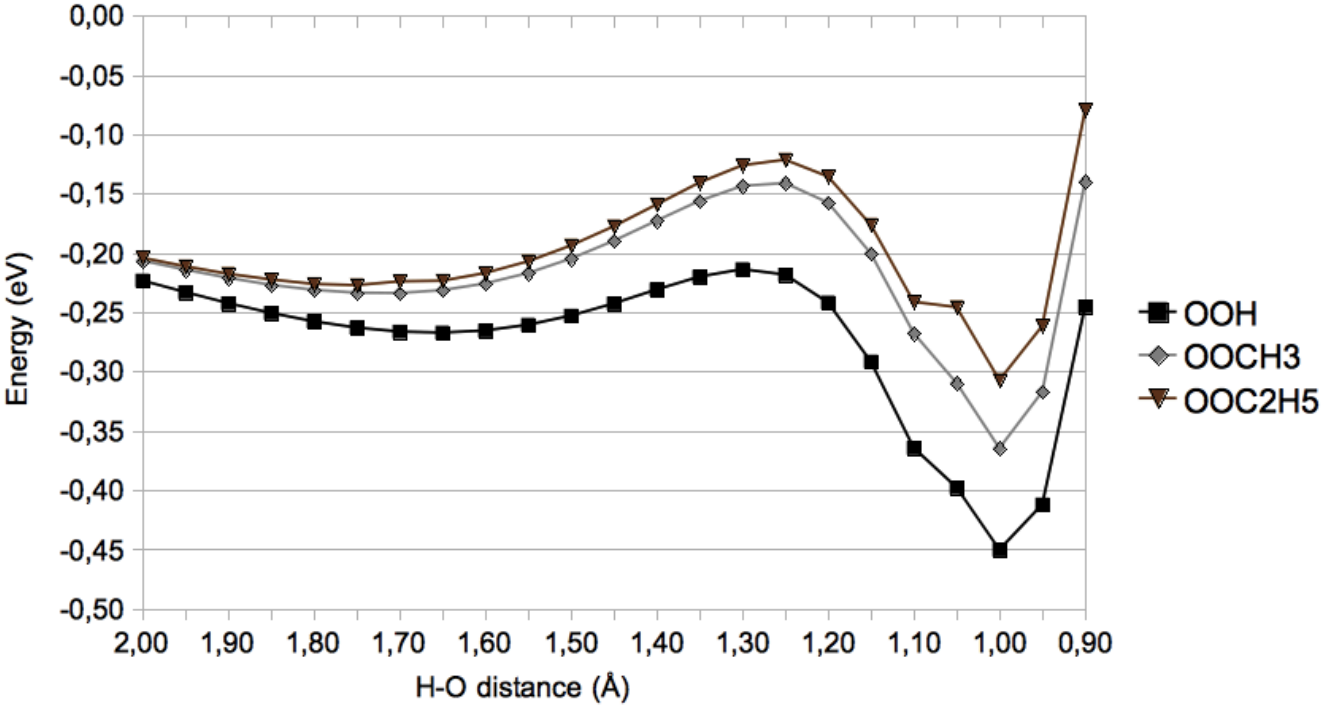

Figure 4.8: *Energy curves for the hydrogen transfer from simplification* **B** *of vitamin E to three different radicals;* $^{\bullet}OOH$, $^{\bullet}OOCH_3$, *and* $^{\bullet}OOC_2H_5$, *calculated with the BLYP functional. The curves show the energy as a function of the distance between the hydrogen in the hydroxyl group and the oxygen in the radical.*

As seen in Fig. (4.8) and Table 4.5, the barrier height for the hydrogen transfer varies depending on the radical. For both functionals, the biggest difference is between $^{\bullet}$OOH and $^{\bullet}OOCH_3$. With the BLYP functional, the barrier height is 83 % larger for the $^{\bullet}OOCH_3$ radical than for the $^{\bullet}$OOH radical, with a difference of 0,043 eV. With the B3LYP functional, the $^{\bullet}OOCH_3$ radical leads to a 25 % higher barrier height than $^{\bullet}$OOH, with 0,077 eV in difference. The difference between the barrier heights for $^{\bullet}OOCH_3$ and $^{\bullet}OOC_2H_5$ is less than this. Here the difference with BLYP is 0,012 eV (13 %) and 0,028 eV (7 %) with B3LYP.

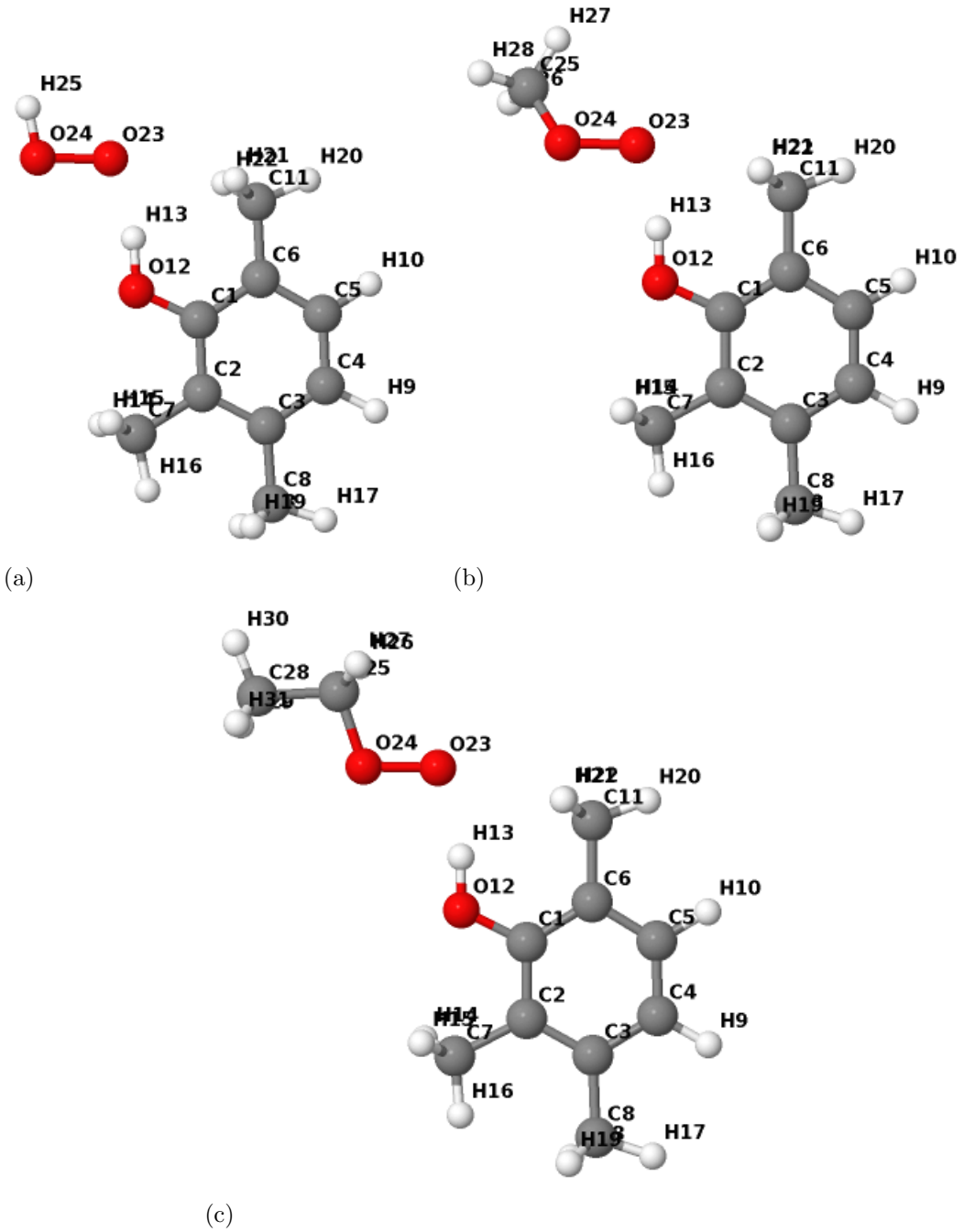

Figure 4.9: *Simplification* **B** *of vitamin E with a hydrogen bond to (a)* $^{\bullet}OOH$*, (b)* $^{\bullet}OOCH_3$*, and (c)* $^{\bullet}OOC_2H_5$*.*

Table 4.5: *Energy barriers for hydrogen transfer from simplification* **B** *to three different radicals with BLYP and B3LYP, and the difference between the two functionals.*

	$^{\bullet}OOH$	$^{\bullet}OOCH_3$	$^{\bullet}OOC_2H_5$
BLYP	0,0515 eV	0,0943 eV	0,1062 eV
B3LYP	0,3058 eV	0,3832 eV	0,4110 eV
Difference	0,2543 eV	0,2889 eV	0,3048 eV

Table 4.6: *Energy difference between the stable system before and after the hydrogen transfer (the reaction energy) from simplification* **B** *to three different radicals for BLYP and B3LYP, and the differences between the two functionals.*

	$^{\bullet}OOH$	$^{\bullet}OOCH_3$	$^{\bullet}OOC_2H_5$
BLYP	0,2634 eV	0,1575 eV	0,0728 eV
B3LYP	0,3741 eV	0,2247 eV	-
Difference	0,1107 eV	0,0672 eV	-

Since $^{\bullet}OOH$ is the most simplified radical compared to the real lipid, and $^{\bullet}OOC_2H_5$ is the least simplified, it is reasonable to believe that the computation with the biggest radical leads to the best value. We can also expect the barrier height for the hydrogen transfer to a lipid to be somewhat larger than for $^{\bullet}OOC_2H_5$, but since the difference is much larger between the two smallest simplifications than between the two largest, a large difference is not expected.

The barrier heights depends even more on the functional used, than on the radical, as seen in Table 4.5. For all three radicals, the barrier height is significantly larger with the B3LYP functional than with the BLYP functional. The smallest numeric difference is with the smallest radical $^{\bullet}OOH$, and the largest with the largest radical $^{\bullet}OOC_2H_5$. The relative difference however, shows that the B3LYP functional results in a barrier height almost 6 times as large as the BLYP functional for $^{\bullet}OOH$, and about 4 times as high for the two other radicals. This is consistent with the results found in section 4.2, and with previous DFT computations on hydrogen barriers [21, 38].

The energy difference between the stable system before and after the hydrogen transfer, the reaction energy, also depends on the radical and the functional used, as seen in both Fig. (4.8) and Table 4.6. For the BLYP functional, the reaction energy is largest with the smallest radical $^{\bullet}OOH$, and smallest with the largest radical $^{\bullet}OOC_2H_5$. The difference is largest between the two smallest radicals, 0,106 eV, and smallest between the two largest radicals, 0,085 eV. The relative

difference is however different, with the reaction energy for the $^{\bullet}OOCH_2$ radical 116% larger than for the $^{\bullet}OOC_2H_5$ radical, and the reaction energy for the $^{\bullet}OOH$ radical 67% larger than for the $^{\bullet}OOCH_2$ radical. For the B3LYP functional, the geometry optimization after the hydrogen transfer to $^{\bullet}OOC_2H_5$ had problems with convergence, and its reaction energy can thus not be found.

Table 4.7: *Mulliken charges for the stable state before the hydrogen transfer from simplification* **B** *to three different radicals, with the BLYP functional. The Mulliken charges for simplification* **B** *without any radical is also included. The names of the different atoms can be seen in Fig. (4.9). The bottom line shows the total charge on the radicals.*

	No radical	$^{\bullet}OOH$	$^{\bullet}OOCH_3$	$^{\bullet}OOC_2H_5$
C1	0,49	0,52	0,52	0,51
O12	-0,54	-0,52	-0,53	-0,53
H13	0,24	0,27	0,27	0,27
O23	-	-0,30	-0,31	-0,32
O24	-	-0,25	-0,19	-0,18
H25	-	0,36	-	-
C25	-	-	0,87	-
H26	-	-	-0,16	-
H27	-	-	-0,16	-
H28	-	-	-0,19	-
C25	-	-	-	0,71
H26	-	-	-	-0,17
H27	-	-	-	-0,17
C28	-	-	-	0,54
H29	-	-	-	-0,17
H30	-	-	-	-0,18
H31	-	-	-	-0,17
Charge radical	-	-0,19	-0,14	-0,12

To summarize, the smallest radical $^{\bullet}OOH$ gives the smallest energy barrier for the hydrogen transfer, and it results in the largest reaction energy. In other words; the hydrogen transfer from simplification **B** to $^{\bullet}OOH$ is the most energy effective reaction with the least activation energy. The two larger systems have larger activation energy and smaller reaction energy. Experimental values for the energy barrier for the reaction of phenol with tert-ButOO$^{\bullet}$ in isopentane is 29,7 kcal/mol (0,31 eV) [34]. Our calculations are not done on the same molecules as this, but the systems are comparable. Since the B3LYP functional results in the energy barriers closest to this value, we assume that this functional produces the best results

for hydrogen transfer calculations. Other DFT/B3LYP studies for the hydrogen transfer from phenol to $^{\bullet}$OOH shows energy barriers of 0,25-0,27 eV [34]. This is consistent with our values found with B3LYP.

We can try to explain this with the Mulliken charges shown in Table 4.7. Without any radical hydrogen bonded to it, the hydroxyl group in simplification **B** is still quite polar, with a negative oxygen atom and a positive hydrogen atom. When a radical is hydrogen bonded to the group, both the hydrogen atom and the carbon atom obtains a larger positive charge, and the oxygen atom a less negative charge. The total charge on the radical when hydrogen bonded to simplification **B** is largest for the smallest radical $^{\bullet}$OOH, where it is -0,19 e. For $^{\bullet}OOCH_3$ the charge is -0,14 e, and the smallest charge is -0,12 e on $^{\bullet}OOC_2H_5$. Thus the electrostatic attraction between the simplification and the radical is larger for $^{\bullet}$OOH than the other two radicals. This can explain why it has the lowest energy barrier, since less energy is needed to start the reaction, as the hydrogen atom already is drawn towards the radical.

4.4.2 Simplification A

Figure (4.10) shows the energy curve for the hydrogen transfer from simplification **A** of vitamin E to two different radicals, $^{\bullet}OOCH_3$ and $^{\bullet}OOC_2H_5$, with the BLYP functional. The molecules at the energy minima before the hydrogen transfer can be seen in Fig. (4.11), with the atom names included. The energy barriers can be seen in Table 4.8 for both the BLYP and B3LYP functional, and the difference in energy of the stable states before and after the hydrogen transfer can be seen in Table 4.9. The Mulliken charges for the stable state before the hydrogen transfer can be seen in Table 4.10.

As mentioned above, simplification **A** with a hydrogen bond to $^{\bullet}$OOH was not stable with the BLYP functional. A geometry optimization of this complex resulted in either a spontaneous hydrogen transfer or a state with the hydrogen in between the simplification and the radical. We therefore concluded that the BLYP functional gives no energy barrier for the hydrogen transfer from simplification **A** to he $^{\bullet}$OOH radical. The B3LYP functional, however, produced a stable state for this complex, and the results from this calculation are included in Table 4.8 and 4.9.

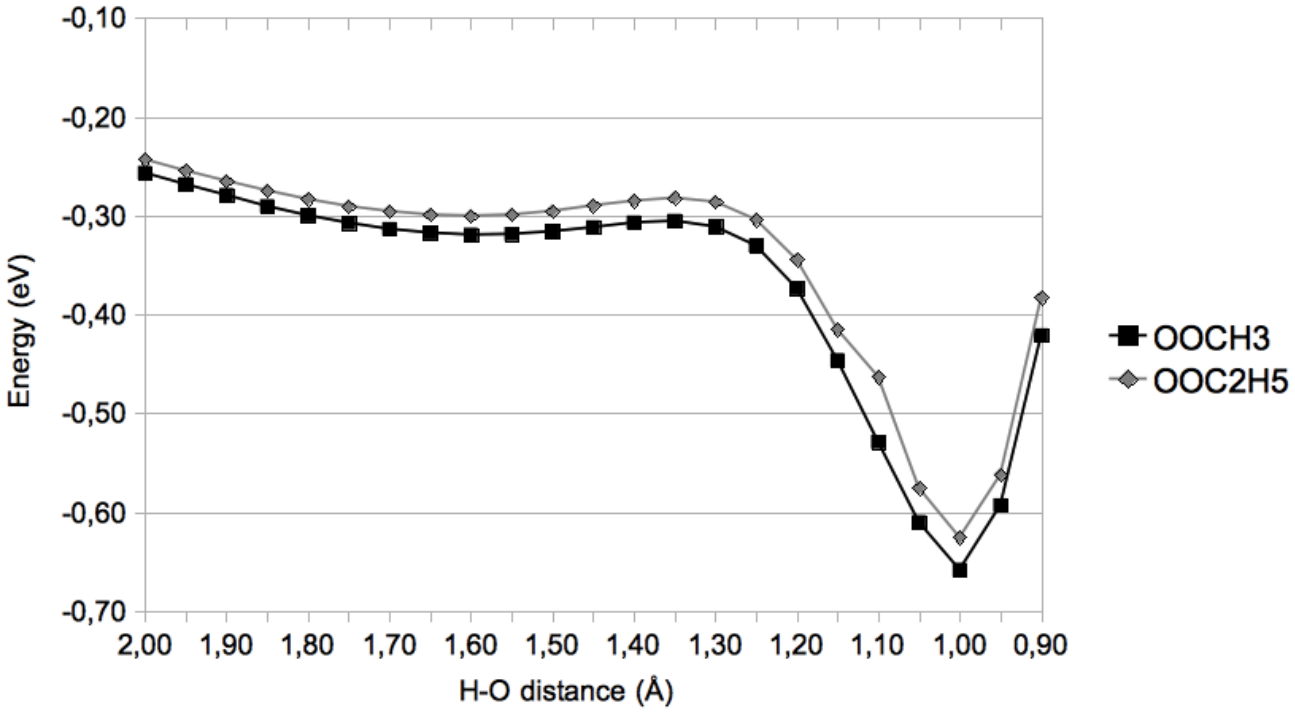

Figure 4.10: *Energy curve for the hydrogen transfer from simplification* **A** *to* $^{\bullet}OOCH_3$ *and* $^{\bullet}OOC_2H_5$ *using the BLYP functional. The curves show the energy as a function of the distance between the hydrogen being transferred and the oxygen on the radical.*

Also for this simplification of vitamin E, the hydrogen transfer to different radicals produces different barrier heights, as can be seen in Fig. (4.10) and Table 4.8. With the BLYP functional, the activation energy for the hydrogen transfer to $^{\bullet}OOC_2H_5$ is 42% larger than for $^{\bullet}OOCH_2$, but the numerical difference is only 0,005 eV. With the B3LYP functional, the same difference is only 8%. The energy barrier for the $^{\bullet}OOCH_3$ radical here, is 48 % larger than for $^{\bullet}OOH$. Since the hydrogen transfer activation energy is so similar for the two largest radicals, it is here even more reasonable to assume that the energy barrier for the hydrogen transfer to the $^{\bullet}OOC_2H_5$ radical is comparable to the hydrogen transfer to a real lipid.

The difference in barrier height produced by the two functionals is also large. The B3LYP functional produces a barrier height 20 and 15 times larger than the BLYP functional for the two largest radicals. While BLYP barrier height is only $\sim$ 0,01 eV, the B3LYP barrier height is $\sim$ 0,20 eV. In [36] the energy barrier calculated for the hydrogen transfer between a molecule similar to simplification **A**

(seen in Fig. 3.1a) and $^{\bullet}$OOH was calculated to 0.18 eV with DFT/B3LYP. This is comparable to the calculated value 0,215 eV with a difference of 0,03 eV. Experimental values are unfortunately not found, but since the B3LYP results were most in comparable to experimental values for simplification **B**, we can assume this is so for simplification **A** as well.

Table 4.8: *Energy barriers for hydrogen transfer from simplification* **A** *to three different radicals with the BLYP and B3LYP functional, and the difference between the two functionals.*

	$^{\bullet}$OOH	$^{\bullet}OOCH_3$	$^{\bullet}OOC_2H_5$
BLYP	0 eV	0,0102 eV	0,0150 eV
B3LYP	0,1455 eV	0,2148 eV	0,2317 eV
Difference	0,1455 eV	0,2082 eV	0,2167 eV

Table 4.9: *Energy difference between the stable system before and after the hydrogen transfer from simplification* **A** *to three different radicals, and the difference between the two functionals used.*

	$^{\bullet}$OOH	$^{\bullet}OOCH_3$	$^{\bullet}OOC_2H_5$
BLYP	-	0,3805 eV	-
B3LYP	0,6560 eV	0,5145 eV	-
Difference	-	0,1340 eV	-

The reaction energy for the hydrogen transfer to $^{\bullet}OOC_2H_5$ can not be found in Fig. (4.9) for any of the functionals. This is because of problems with convergence caused by the $HOOC_2H_5$ molecule which have no constraints for its placement relative to simplification (**A**). Similar problems were also experienced with simplification (**B**), but for that case convergence could be obtained. We can however see that the reaction energy for the $^{\bullet}$OOH radical is larger than for the $^{\bullet}OOCH_3$ radical, and according to Fig. (4.10), the energy curves for $^{\bullet}OOC_2H_5$ and $^{\bullet}OOCH_3$ are very similar.

The Mulliken charges (Table 4.10) shows that the $^{\bullet}OOCH_3$ has a slightly more negative charge than $^{\bullet}OOC_2H_5$ does when hydrogen bonded to simplification A, but the difference is very small. Also here, as for simlification **B**, the charge on the hydrogen atom in the hydroxyl group and the carbon atom becomes more positive when hydrogen bonded to a radical, while the oxygen atom becomes slightly less negative. The group is however slightly more polarized when bonded to a radical, and we can expect a attractive force between the hydrogen atom in the hydroxyl group and the radical.

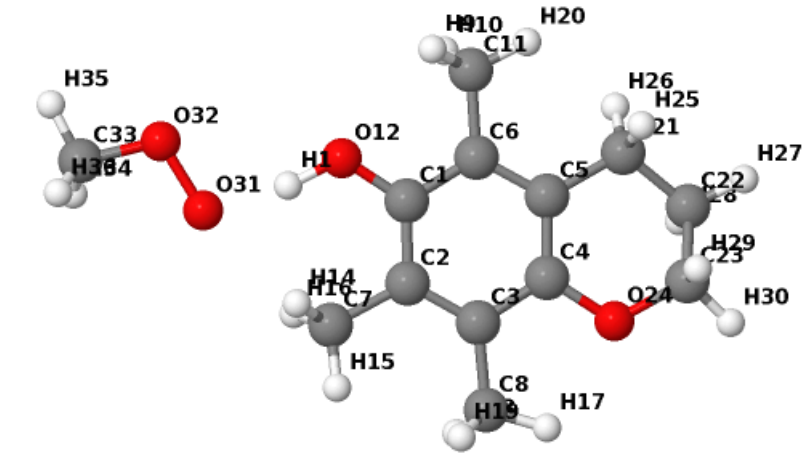

(a)
$OOCH_3$

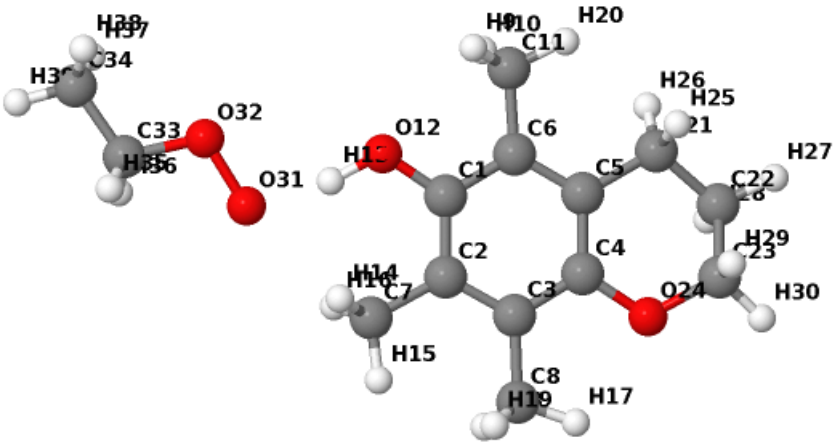

(b)
OOC_2H_5

Figure 4.11: *Simplification* **A** *of vitamin E with a hydrogen bond to (a)* $^{\bullet}OOCH_3$ *and (b)* $^{\bullet}OOC_2H_5$.

Table 4.10: *Mulliken charges for the geometry optimized state before the hydrogen transfer from simplification* **A** *to* $^{\bullet}OOCH_3$ *and* $^{\bullet}OOC_2H_5$*, with the BLYP functional. The charges on simplification* **A** *without any radical are also included. The atom numbers can be found in Fig. (4.11). The bottom line shows the total charge for the radical.*

	No radical	$^{\bullet}OOCH_3$	$^{\bullet}OOC_2H_5$
C1	0,47	0,52	0,52
O12	-0,55	-0,54	-0,54
H13	0,24	0,27	0,27
O31	-	-0,36	-0,36
O32	-	-0,23	-0,22
C33	-	0,89	-
H34	-	-0,17	-
H35	-	-0,20	-
H36	-	-0,17	-
C33	-	-	0,73
H26	-	-	0,53
H27	-	-	-0,18
C28	-	-	-0,18
H29	-	-	-0,17
H30	-	-	-0,17
H31	-	-	-0,19
Charge radical	-	-0,24	-0,23

4.5 Simplification A versus B

As seen above, there is a lot of differences between simplification **A** and **B**. Since simplification **A** is the least simplified version of vitamin E, we can expect it to produce the results closest to vitamin E. This is also confirmed in previous work done on vitamin E-like molecules [9]. As mentioned above, the only difference between the two simplifications is the heterocyclic ring which is replaced by two hydrogen atoms in simplification **B**. The explanations to the differences are therefore probably assigned to this heterocyclic ring.

By comparison of Table 4.5 and 4.8, we can clearly see that the energy barriers for simplification **A** are much smaller than for simplification **B**. For the $^{\bullet}OOH$ radical, the energy barrier with BLYP on simplification **A** is zero. These results show that simplification **A** is more reactive than simplification **B**, since it more

easily donates the hydrogen atom to a radical. This is in agreement with the work done in [9], where a molecule comparable to simplification **B** was found to be far less reactive than a molecule comparable to simplification **A**. Also for the rotation of the hydroxyl group, simplification **A** results in a lower energy barrier than simplification **B**. In general, the hydrogen atom can be assumed to be more loosely bonded to simplification **A** than to simplification **B**.

The energy differences between the geometry optimized state before and after the hydrogen transfer are also different for the two simplifications (Table 4.6 and 4.9). The final state are more stable than the state before the hydrogen transfer for both simplifications, but the energy difference is much larger for simplification **A** than for **B**. This also implies that the hydrogen transfer is more favorable for simplification **A** than for **B**.

The Mulliken charges for the stable states before the hydrogen transfer for the two simplifications in Table 4.7 and 4.10 can give us an indication about the energy barrier differences. Although the differences are small, the total charge on the carbon, oxygen and hydrogen on the simplifications without any radical on simplification **A** are more negative than on simplification **B**. When a radical is added, the differences gets much more apparent. The charges on the carbon, oxygen and hydrogen in total are much the same for the two simplifications, but the total charge on the radicals gets significantly more negative (about 0,1 e) for simplification **A** than for **B**. This implies that the heterocyclic ring on simplification **A** is an electron donating group, and this is probably one of the reasons why simplification **A** is more reactive than simplification **B**. Studies with different substituents for the phytyl tail on vitamin E shows that the antioxidant activity increases with electron donating substituents [36]. This is consistent with our assumption that the heterocyclic ring is an electron donating group, since it increases the antioxidant activity of vitamin E.

Another difference between the two simplifications, is the O-H bond lengths and the hydrogen bond lengths (Table 4.11). We can see that without a radical, the O-H bond length is the same for both simplifications. This bond length increases in some extent (0,03-0,06 Å) when the simplification is hydrogen bonded to a radical, and the H-O bond length increases more for simplification **A** than for **B**. The biggest difference lies in the length of the hydrogen bond, where this length is about 0,15 Å shorter for simplification **A** than for **B**. Table 4.2 and 4.3 also confirms that the hydrogen bonds are stronger for simplification **A** than for **B**.

Table 4.11: *Bond lengths for O-H bond and hydrogen bond on both simplifications hydrogen bonded to radicals.*

Simplification	Bond type	No radical	$^{\bullet}OOH$	$^{\bullet}OOCH_3$	$^{\bullet}OOC_2H_5$
A	O-H	0,97 Å	-	1,03 Å	1,03 Å
	hydrogen	-	-	1,55 Å	1,56 Å
B	O-H	0,97 Å	1,01 Å	1,00 Å	1,00 Å
	hydrogen	-	1,63 Å	1,70 Å	1,70 Å

The difference between the bond lengths can be a result of the difference in the Mulliken charges on the radicals. The radicals hydrogen bonded to simplification **A** are more negative than those hydrogen bonded to simplification **B**, and this will result in a larger attraction between the hydroxyl group and the radical for simplification **A**. This again may lead to a shorter hydrogen bond between the components, and the hydrogen transfer occurs more easy.

4.6 Exchange correlation functionals

As can be seen for both the simplifications, the B3LYP functional results in higher energy barriers and a larger reaction energy for hydrogen transfers. The difference is however not so large for the rotation of the hydroxyl group. This confirms what other studies shows, that many exchange correlation functionals have problems predicting the right energy barrier for hydrogen transfer calculations [20, 21].

Many explanations for the problems for the pure DFT functional have been given. Some concludes that the main difficulties lie in the fundamental deficiencies of the DFT model. [21]. Johnsen, Gonzales, Gill and Pople have studied the reaction $H+H_2 \rightarrow H_2+H$ with 24 different DFT methods [38]. Comparing with experimental values, they concluded that the error in the barrier heights in DFT calculations may lie in self-interaction. The addition of self-interaction correction seemed to give an energy change in the proper direction. Baker et al. however, suggested that the error for pure DFT computations is caused by the Slater exchange term [20]. The hybrid functionals are able to correct for some of those deficiencies.

For hydrogen transfers from simplification **B**, the barrier heights calculated was in reasonable agreement with experimental values. We can therefor assume that the B3LYP functional yields better results than the BLYP functional for these hydrogen transfer calculations. With the BHandHLYP functional, even higher barrier heights were found. This functional includes a larger amount of Hartree Fock exact exchange than B3LYP. We therefore assume that the HF exact exchange increases the barrier height.

4.7 Rotation of hydroxyl group when hydrogen bonded to different radicals

There has also been done a rotation of the hydroxyl group hydrogen bonded to two different radicals, $^{\bullet}$OOH and $^{\bullet}$OOCH$_3$. The result of this rotation can be seen in Fig. (4.12). The rotation is done on the α-isoform of simplification **B** with the BLYP functional.

For the rotation of the hydroxyl group hydrogen bonded to the $^{\bullet}$OOH radical, a sudden drop in energy can be seen at 110 degrees, right after the transition state for the rotation. This drop is caused by a spontaneous hydrogen transfer from the vitamin E simplification to the radical, creating a HOOH molecule bonded to a vitamin E-radical. With $^{\bullet}$OOCH$_3$, the hydrogen atom on the hydroxyl group does not transfer to $^{\bullet}$OOCH$_3$, causing no energy drop in the energy curve.

The different barrier heights for hydrogen transfer from simplification **B** to $^{\bullet}$OOH and $^{\bullet}$OOCH$_3$ can explain the different results this rotation has. With energies 0,052 eV and 0,094 eV respectively, the hydrogen transfer to $^{\bullet}$OOCH$_3$ has almost twice the energy barrier as to $^{\bullet}$OOH. The excitation of the hydroxyl group away from its ground state was therefore enough to make the hydrogen transfer happen for $^{\bullet}$OOH, but not for $^{\bullet}$OOCH$_3$.

Simplification **A** has a lower energy barrier than simplification **B**. Actually, for the BLYP functional, the lowest energy barrier for simplification **B** is larger than the largest energy barrier for simplification **A**. If the hydroxyl group is rotated out of the plane, it is therefore probable that this spontaneous hydrogen transfer will happen for all the radicals tested here with the BLYP functional on simplification **A**. The B3LYP functional produces a larger energy barrier, so it is not that probable that a hydrogen transfer will happen for B3LYP calculations.

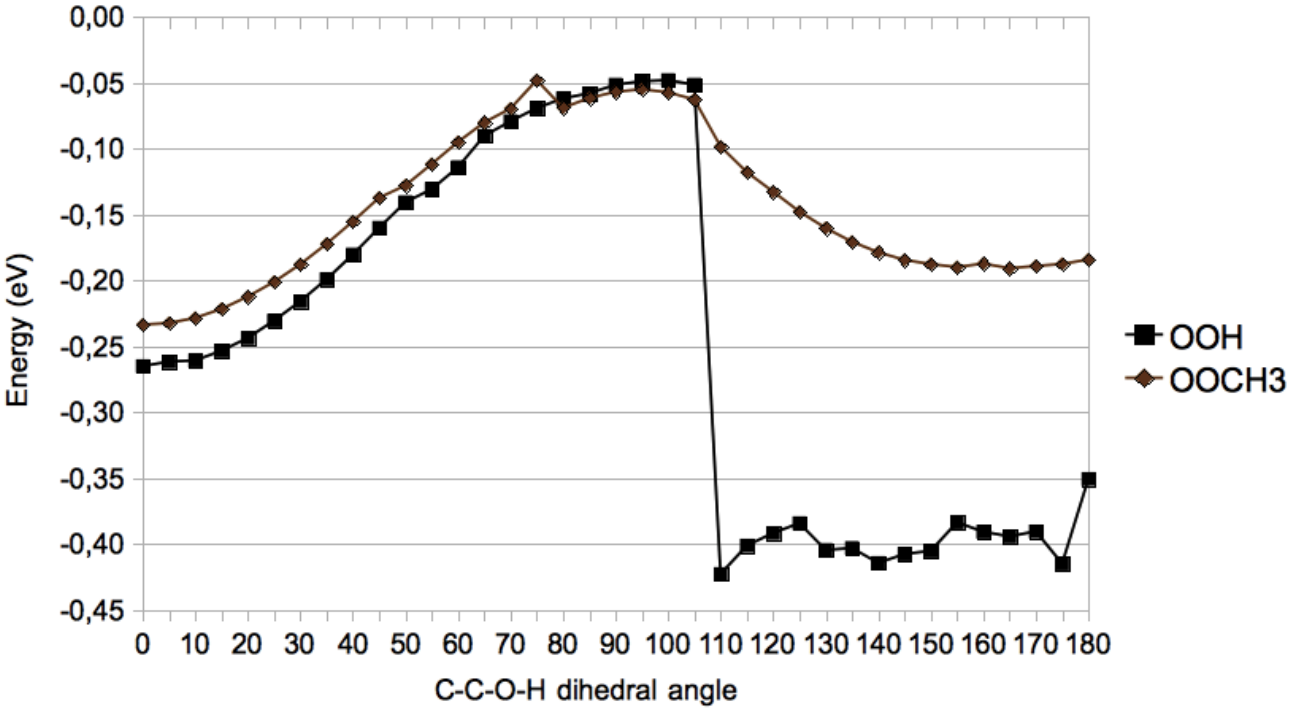

Figure 4.12: *Energy curve for rotation of hydroxyl group when hydrogen bonded to $^{\bullet}OOH$ and $^{\bullet}OOCH_3$ with the BLYP functional. The curves show the energy as a function of the C-C-O-H dihedral angle.*

The α-isoform has the lowest energy barriers for rotation of the hydroxyl group. We have mentioned that this may be a reason why this isoform is the most biological active of the different vitamin E isoforms. The hydrogen transfer reaction happens spontaneous when the hydroxyl group hydrogen bonded to $^{\bullet}$OOH is rotated away from the ground state. The hydrogen transfer from the transition state of this rotation thus can be assumed to have a lower energy barrier than the hydrogen transfer from the ground state. A low energy barrier for rotation out of the ground state energy increase the probability that the hydroxyl group can be found at the transition state. This increases the probability that a hydrogen transfer happens from this state, and the reactivity of the molecule increases.

4.8 Error discussion

This is a DFT study of vitamin E-like molecules, and not an experimental study. We therefore have no guarantee that the results obtained are correct. We have however observed that the results from the hydrogen transfer calculations matches some previous work done in the field. This gives an indication a certain reliability of the results obtained.

With the BLYP functional, every maximum and minimum energy could be validated with frequency calculations. If an unwanted imaginary frequency was obtained, the coordinate causing this frequency was changed, and a new geometry optimization or transition state search was run until none or one imaginary frequency was obtained. This way we can be sure that the geometries found are correct. We can however not be sure that it is the global energy minima or the only and lowest transition state. For a selection of the geometries resulting in energy minima, a test for this has been run by changing atomic coordinates and run a new geometry optimization. Some coordinates have also been rotated with a linear transit run. For all these tests, the original geometry always provided the lowest energy. We can however not know that this is the case for all geometries, but it strengthens the possibility that it is so.

With the B3LYP functional, such a frequency calculation is not available with ADF. However, when doing the B3LYP calculations, the initial geometry used was always the geometry from the BLYP calculation on the same system. After convergence with the B3LYP functional was obtained, the geometry and energy changes were checked not to be too large. This way we obtain a certain assurance that an actual energy minima or maxima is found.

An other error is the Mulliken charges. As mentioned previously, the Mulliken charges are very basis set dependent [33]. We have used the same basis set for all calculations, so though the obtained charges can not be compared directly with experimental values, they can be compared with each other for different systems as we have done. We can neither be sure that they are exact, but we can assume that they illustrate a trend.

For all calculations, the initial geometry was the global energy minima. However, the local energy minima also yields a stable geometry. A hydrogen transfer can also happen from this state. For some isoforms the energy difference between the local and global energy minima are quite big. For the α-isoform of simplification **A**, the difference is $\tilde{0}$,03 eV, or 25 % of the energy barrier for the rotation of the hydroxyl group from the global energy minima. Since a hydrogen transfer from the transition state results in a lower energy barrier, it is probable that a hydrogen transfer from the local energy minima also does so. This way the energy barrier found is probably the biggest one, and other initial approaches will maybe lead to other energy barriers.

Chapter 5

Summary and conclusions

We have studied the antioxidant property of two vitamin E simplifications with density functional theory. In one of the simplifications, the phytyl tail and the methyl group on the heterocyclic ring in vitamin E is replaced by two hydrogen atoms, simplification **A**. In the other simplification the heterocyclic ring is replaced by two hydrogen atoms, simplification **B**.

First, a rotation of the hydroxyl group in the two simplifications were carried out for five isoforms of vitamin E. The energy minima for all isoforms of both simplifications were found to be when the the hydroxyl group was placed in the same plane as the aromatic ring, and the transition state when the group is perpendicular to the aromatic plane. For both simplifications, the α-isoform resulted in the lowest rotational barriers, and the barrier heights were significantly lower for simplification **A** than for **B**; 0,116 eV versus 0,162 eV for the BLYP functional, and 0,104 eV versus 0,136 eV with the B3LYP functional. For simplification **B**, the geometry with the hydroxyl group pointing towards the side with the fewest methyl groups or with the methyl group furthest away resulted in the global energy minima. For simplification **A**, the geometry with the hydroxyl group pointing away from the heterocyclic ring resulted in the global minimum point for all isoforms.

A hydrogen transfer from the α-isoform of the simplified versions of vitamin E to three different radicals, $^{\bullet}OOH$, $^{\bullet}OOCH_3$, and $^{\bullet}OOC_2H_5$, have also been carried out. For the largest radical, this resulted in barrier heights of 0,106 eV and 0,411 eV for simplification **B**, and 0,015 eV and 0,232 eV for simplification **A**, calculated with the BLYP and B3LYP exchange correlation functionals respectively. The hydrogen transfer barriers for simplification **B** are found to be much larger than for

simplification **A**, while the reaction energy for simplification **A** is found to be much larger than for simplification **B**. Thus the hydrogen transfer from simplification **A** is much more probable than from simplification **B**. The different radicals also resulted in different barrier heights, with larger barriers for larger radicals. The energy barrier for the hydrogen transfer from simplification **A** fits with energy barriers found for similar systems in earlier studies.

Since the only differences between the two simplifications is the heterocyclic ring, this is concluded to be the reason for the differences obtained. The heterocyclic ring is concluded to be an electron donor, since the Mulliken charges on the radicals that are hydrogen bonded to the hydroxyl group are much more negative for simplification **A**, than for **B**. For simplification **A**, the O-H bond gets more stretched than for simplification **B**, and the hydrogen bond length is shorter in the stable state before the hydrogen transfer. The binding energies are also found to be larger for simplification **A** than for **B**. Simplification **A** hydrogen bonded to $^{\bullet}OOC_2H_5$ has a binding energy of 0,297 eV, while the same radical hydrogen bonded to simplification **B** has a binding energy of 0,227 eV.

We have also seen that the three exchange correlation functionals BLYP, B3LYP, and BHandHLYP provide very different results. For all hydrogen transfers, the B3LYP functional results in many times as high activation energy as the BLYP functional. The single test run with the BHandHLYP functional resulted in an even higher energy barrier. Since both B3LYP and BHandHLYP includes Hartree Fock exact exchange, and BHandHLYP more so than B3LYP, this is concluded to be the reason for this difference. These results also fit with previous results. For rotation of the hydroxyl group, the B3LYP functional results in slightly smaller energy barriers than the BLYP functional.

We can conclude that the most simplified molecule, simplification **B**, is a poor model for vitamin E. It is far less reactive than simplification **A**, and thus a poorer antioxidant.

Chapter 6

Future work

This section gives suggestions for future work. This project has run over a finite amount of time, so not all interesting investigations has been done. In this project, only hydrogen transfers from the α-isoform has been run. It would for instance be interesting to investigate the energy barriers for the hydrogen transfer from other isoforms than the α-isoform. This could show and maybe indicate why the α-isoform is the most reactive isoform. Hydrogen transfer from the local energy minima could also prove interesting to see how much the orientation of the hydroxyl group has to say for the reactivity of the molecule. The main interest as we see it would however be to investigate further the relationship between the hydrogen transfer barrier heights and the C-C-O-H dihedral angle for the hydroxyl group. We have seen indications that the energy barrier decreases when the hydroxyl group is in a transition state, but this is not proved.

References

[1] G. Wolf, "The discovery of the antioxidant function of vitamin E: the contribution of Henry A. Mattill," *The Journal of nutrition*, vol. **135**, pp. 363–366, (2005).

[2] A. Kamal-Eldin and L.-Å. Appelqvist, "The Chemistry and Antioxidant Properties of Tocopherols and Tocotrienols," *Lipids*, vol. **31**, pp. 671–701, (1996).

[3] Office of Dietry Supplements, "Dietary Supplement Fact Sheet: Vitamin E." (Office of Dietary Supplements, National Institutes of Health Clinical Center, National Institutes of Health, Bethesda). Available at http://ods.od.nih.gov/factsheets/vitamine/.

[4] L. Packer, S. U. Weber, and G. Rimbach, "Molecular Aspects of α-Tocotrienol Antioxidant Action and Cell Signalling," *The Journal of Nutrition*, vol. **131**, pp. 369S–373S, (2001).

[5] S. Nagaoka, T. Kakiuchi, K. Ohara, and K. Mukai, "Kinetics of the reaction by which natural vitamin E is regenerated by vitamin C," *Chemistry and physics of lipids*, vol. **146**, pp. 26–32, (2007).

[6] E. Klein, V. Lukeš, and M. Ilčin, "DFT/B3LYP study of tocopherols and chromans antioxidant action energetics," *Chemical physics*, vol. **336**, pp. 51–57, (2007).

[7] X. Wang and P. J. Quinn, "Vitamin E and its function in membranes," *Progress in Lipid Research*, vol. **38**, pp. 309–336, (1999).

[8] R. Brigelius-Flohé, "Vitamin E: the shrew waiting to be tamed," *Free Radical Biology and Medicine*, vol. **46**, pp. 543–554, (2009).

[9] G. W. Burton and K. U. Ingold, "Autoxidation of biological molecules. 1. Antioxidant activity of vitamin E and related chain-breaking phenolic antioxidants in vitro," *Journal of the American Chemical Society*, vol. **103**, pp. 6472–6477, (1981).

[10] G. Burton and K. Ingold, "Vitamin E: application of the principles of physical organic chemistry to the exploration of its structure and function," *Accounts of Chemical Research*, vol. **19**, pp. 194–201, (1986).

[11] S. Skivastava, R. S. Phadke, G. Govil, and C. N. R. Rao, "Fluidity, Permeability and Antioxidant Behaviour of Model Membranes Incorporated with α-Tocopherol and Vitamin E Acetate," *Biochimica et Biophysica Acta*, vol. **734**, pp. 353–362, (1983).

[12] L. Packer, "Protective role of vitamin E in biological systems," *American Journal of Clinical Nutrition*, vol. **53**, pp. 1050S–1055S, (1991).

[13] J. S. Wright, E. R. Johnson, and G. A. DiLabio, "Predicting the Activity of Phenolic Antioxidants: Theoretical Method, Analysis of Substituent Effects, and Application to Major Families of Antioxidants," *Journal of the American Chemical Society*, vol. **123**, pp. 1173–1183, (2001).

[14] H. Zhang and H. Ji, "How vitamin E scavenges DPPH radicals in polar protic media," *New Journal of Chemistry*, vol. **30**, pp. 503–504, (2006).

[15] R. E. Beyer, "The Role of Ascorbate in Antioxidant Protection of Biomembranes: Interaction with Vitamin E and Coenzyme Q," *Journal of Bioenergetics and Biomembranes*, vol. **26**, pp. 349–358, (1994).

[16] O. Brede, M. R. Ganapathi, S. Naumov, W. Naumann, and R. Hermann, "Localized Electron Transfer in Nonpolar Solution: Reaction of Phenols and Thiophenols with Free Solvent Radical Cations," *The Journal of Physical Chemistry*, no. **105**, pp. 3757–3764, (2001).

[17] O. Brede, R. Hermanna, W. Naumann, and S. Naumov, "Monitoring of the Heterogroup Twisting Dynamics in Phenol Type Molecules via Different Characteristic Free-Electron-Transfer Products," *The Journal of Physical Chemistry*, vol. **106**, pp. 1398–1405, (2002).

[18] O. Brede, S. Naumov, and R. Hermann, "Monitoring molecule dynamics by

free electron transfer," *Radiation Physics and Chemistry*, vol. **67**, pp. 225–230, 2003.

[19] Y. Zhao and D. Truhlar, "Density Functionals with Broad Applicability in Chemistry," *Accounts of chemical research*, vol. **41**, pp. 157–167, (2008).

[20] J. Baker, J. Andzelm, M. Muir, and P. R. Taylor, "OH+H_2 →H_2O+H. The importance of "exact exchange" in density functional theory," *Chemical Physics Letters*, vol. **237**, pp. 53–60, (1995).

[21] M. Nguyen, S. Creve, and L. Vanquickenborne, "Difficulties of density functional theory in investigating addition reactions of the hydrogen atom," *The Journal of Physical Chemistry*, vol. **100**, pp. 18422–18425, (1996).

[22] P. C. Hemmer, *Kvante mekanikk.* Tapir Akademiske Forlag, 4th ed., (2000).

[23] A. Leach, *Molecular modelling: principles and applications.* Pearson Education Limited, 2nd ed., (2001).

[24] J. Slater, "The theory of complex spectra," *Physical Review*, vol. **34**, pp. 1293–1322, (1929).

[25] N. Argaman and G. Makov, "Density functional theory - An introduction," *American Journal of Physics*, vol. **68**, pp. 69–79, (2000).

[26] L. H. Thomas, "The calculation of atomic fields," *Mathematical Proceedings of the Cambridge Philosophical Society*, vol. **27**, pp. 542–548, (1927).

[27] E. Fermi, "Un metodo statistico per la determinazione di alcune proprietà dell'atomo," *Rendiconti dell'Accademia dei Lincei*, no. **6**, pp. 602–607, (1927).

[28] P. Hohenberg and W. Kohn, "Inhomogeneous Electron Gas," *Physical Review*, vol. **136**, pp. B864–B871, (1964).

[29] D. S. Sholl and J. A. Steckel, *Density Functional Theory. A Practical Introduction.* Wiley, (2009).

[30] W. Kohn and L. J. Sham, "Self-Consistent Equations Including Exchange and Correlation Effects," *Physical Review*, vol. **140**, pp. A1133–A1138, (1965).

[31] A. Becke, "A new mixing of Hartree-Fock and local density-functional theories," *The Journal of chemical physics*, vol. **98**, pp. 1372–1377, (1993).

[32] Scientific Computing & Modelling NV, "Adf user's guide." http://www.scm.com/Doc/Doc2010/ADF/ADFUsersGuide/ADFUsersGuide.pdf, (2010).

[33] G. te Velde, F. Bickelhaupt, E. Baerends, C. Fonseca Guerra, S. van Gisbergen, J. Snijders, and T. Ziegler, "Chemistry with ADF," *Journal of Computational Chemistry*, vol. **22**, pp. 931–967, (2001).

[34] V. B. Luzhkov, "Mechanisms of antioxidant activity: The DFT study of hydrogen abstraction from phenol and toluene by the hydroperoxyl radical," *Chemical Physics*, vol. **314**, pp. 211–217, (2005).

[35] O. Tishchenko, D. G. Truhlar, A. Ceulemans, and M. T. Nguyen, "A unified perspective on the hydrogen atom transfer and proton-coupled electron transfer mechanisms in terms of topographic features of the ground and excited potential energy surfaces as exemplified by the reaction between phenol and radicals," *Journal of the American Chemical Society*, vol. **130**, pp. 7000–7010, (2008).

[36] S. Gutiérrez-Oliva, "Theoretical study of the hydrogen abstraction from vitamin-E analogues. The usefulness of DFT descriptors," *Journal of Molecular Modeling*, vol. **17**, pp. 593–598, (2011).

[37] J. S. Wright, D. J. Carpenter, D. J. McKay, and K. U. Ingold, "Theoretical Calculation of Substituent Effects on the O-H Bond Strength of Phenolic Antioxidants Related to Vitamin E," *Journal of the American Chemical Society*, vol. **119**, pp. 4245–4252, (1997).

[38] B. Johnson, C. Gonzales, P. Gill, and J. Pople, "A density functional study of the simplest hydrogen abstraction reaction. Effect of self-interaction correction," *Chemical physics letters*, vol. **221**, pp. 100–108, (1994).

[39] P. E. Siegbahn, M. R. Blomberg, and R. H. Crabtree, "Hydrogen transfer in the presence of amino acid radicals," *Theoretical Chemistry Accounts: Theory, Computation, and Modeling (Theoretica Chimica Acta)*, vol. **97**, pp. 289–300, (1997).

List of Tables

List of Figures

Appendix A

Molecules used

All molecules used to do the computations are pictured below in their ground state. Figure A.1 shows the three hydroperoxides both as radicals and after they has been reduced. Figure A.2 shows all the five isoforms of simplification **B** of vitamin E. Figure A.3 shows the α- and δ- isoform of simplification **A** together with the simplification without any methyl groups. Finally, in figure A.4, the two radicals of the α-isoform of simplification **A** and **B** can be found.

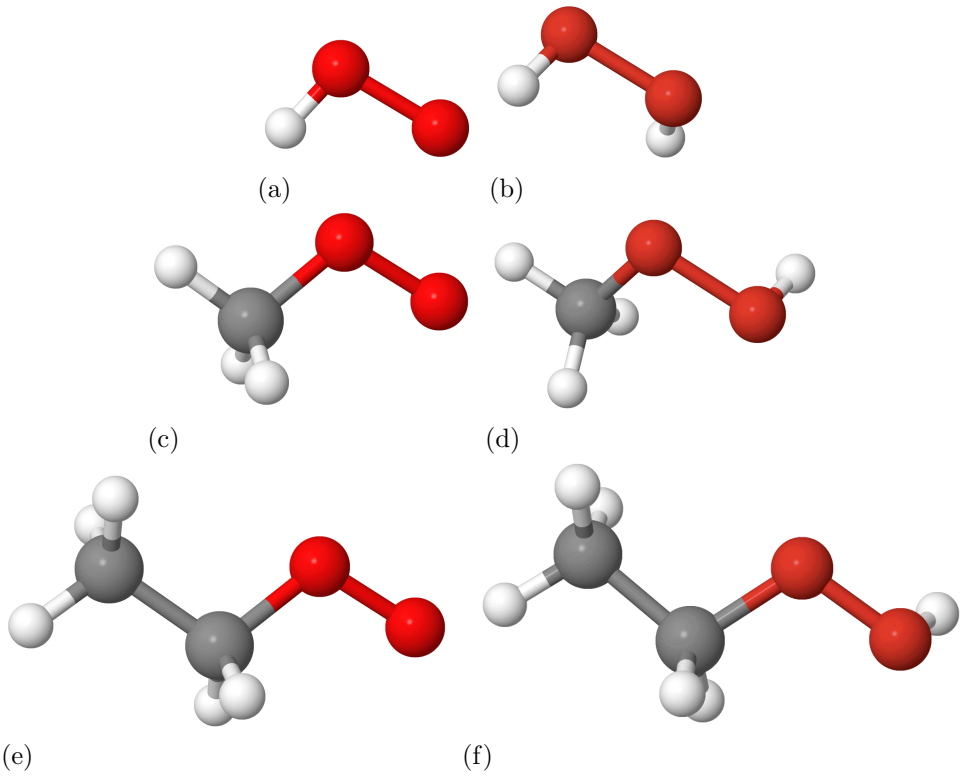

Figure A.1: *The three used hydorperoxides in their ground state; (a) $^{\bullet}OOH$-radical and the reduced (b) $HOOH$, (c) $^{\bullet}OOCH_3$-radical and the reduced (d) $HOOVH_3$, (e) $^{\bullet}OOC_2H_5$-radical and the reduced $HOOC_2H_5$.*

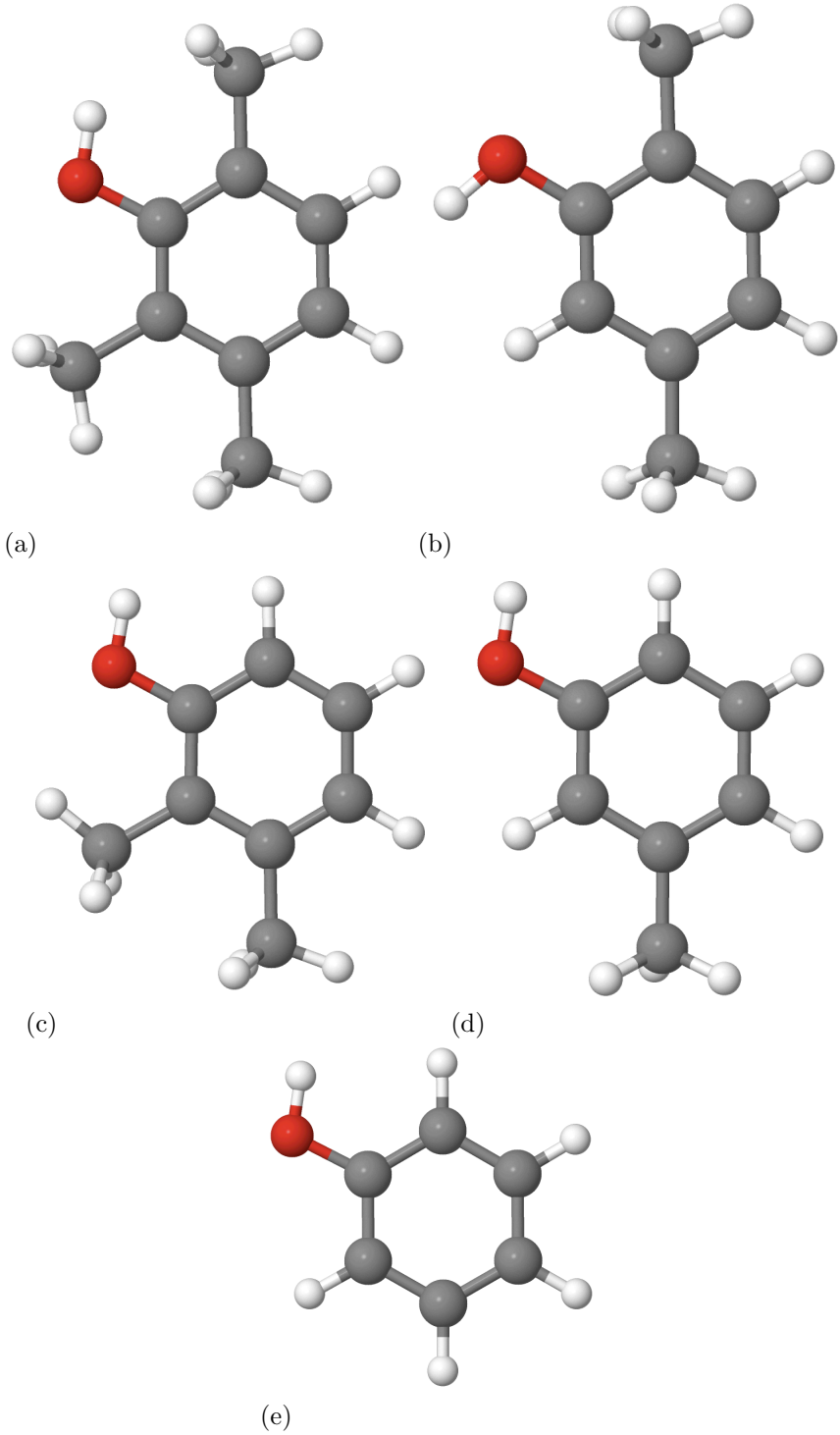

Figure A.2: *The five isoforms of simplification* **B** *of vitamin E in their ground state; (a) the α-isoform, (b) the β-isoform, (c) the γ-isoform, (d) the δ-isoform, and (e) the isoform without any methyl groups, i.e. phenol.*

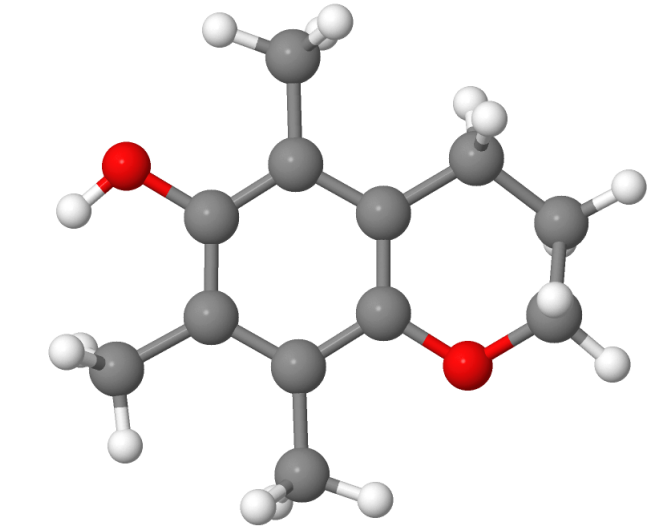

(a)

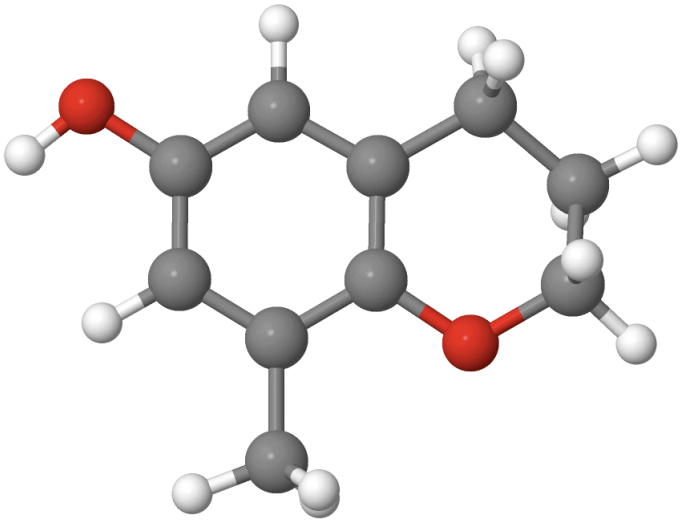

(b)

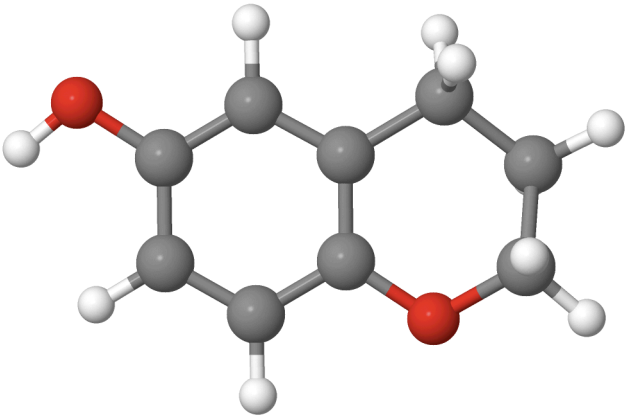

(c)

Figure A.3: *The three used isoforms of simplification* **A** *of vitamin E in their ground state; (a) the α-isoform, (b) the δ-isoform, and (c) the isoform without any methyl groups.*

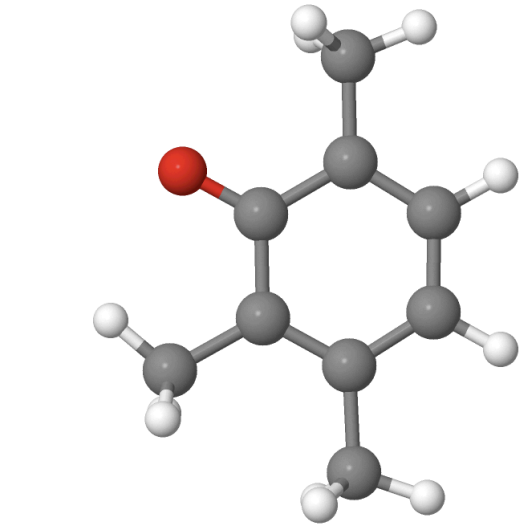

(a)

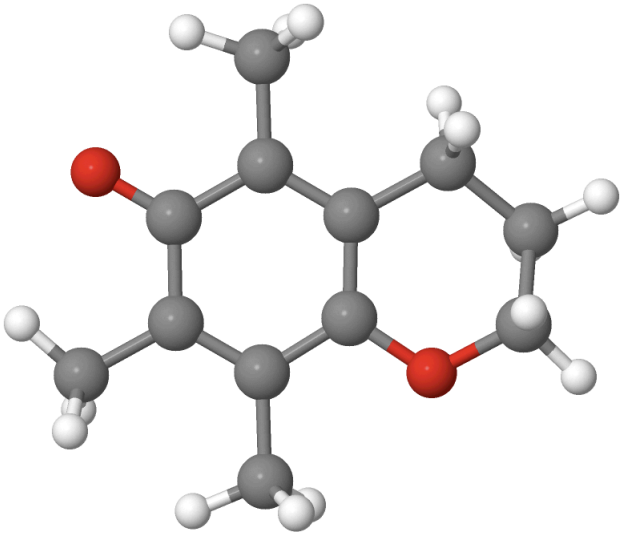

(b)

Figure A.4: *The vitamin E simplification radical, after donation of the hydrogen atom in the hydroxyl group. (a) Simplification* **B**. *(b) Simplification* **A**.

Appendix B

Hydrogen transfer from simplification with one ring to OOH

Figure B.1 shows every second step of the linear transit hydrogen transfer from simplification B to $^{\bullet}OOH$. The distance between the radical and the hydrogen in the hydroxyl group decreases 0.1 Å for every geometry, from 2.0 Å to 0.9 Å. This is the results from the same calculation as in figure 4.8.

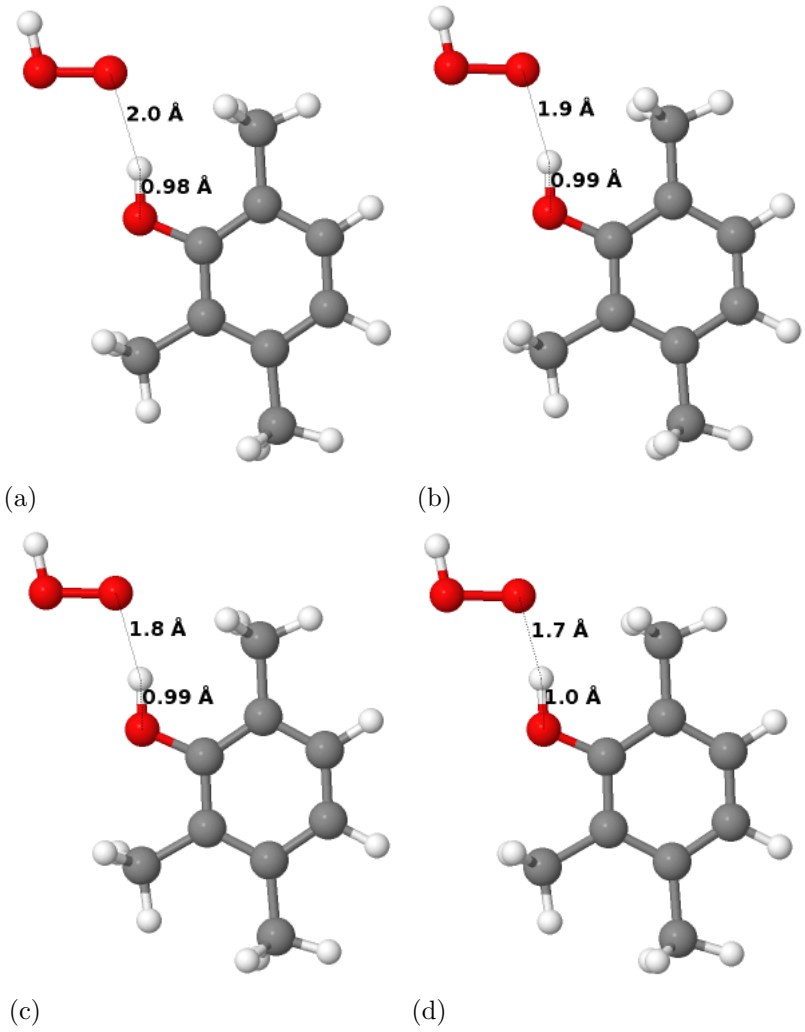

Figure B.1: *Geometries for the hydrogen transfer from simplification B to $^{\bullet}OOH$ seen in figure 4.8. The hydrogen bond length between the hydrogen atom in the hydroxyl group and the oxygen in the radical is (a) 2,00 Å, (b) 1,90 Å, (c) 1,80 Å, and (d) 1,70 Å.*

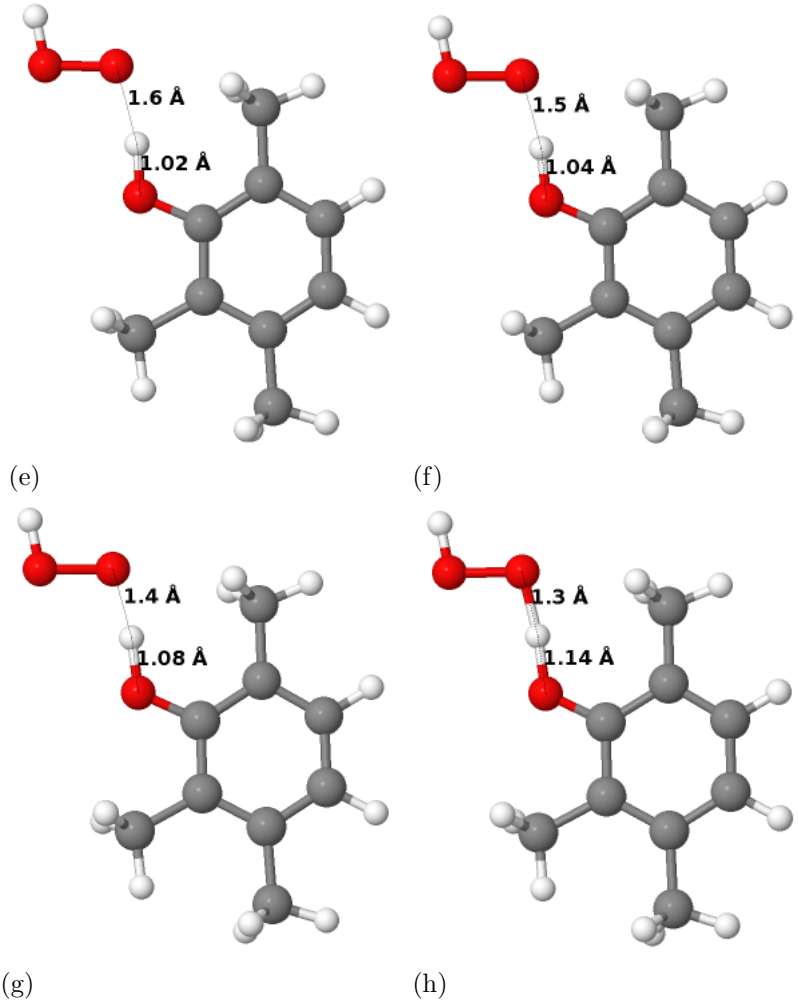

(e) (f)

(g) (h)

Figure B.1: *Geometries for the hydrogen transfer from simplification B to $^{\bullet}OOH$ seen in figure 4.8. The hydrogen bond length between the hydrogen atom in the hydroxyl group and the oxygen in the radical is (e) 1,60 Å, (f) 1,50 Å, (g) 1,40 Å, and (h) 1,30 Å.*

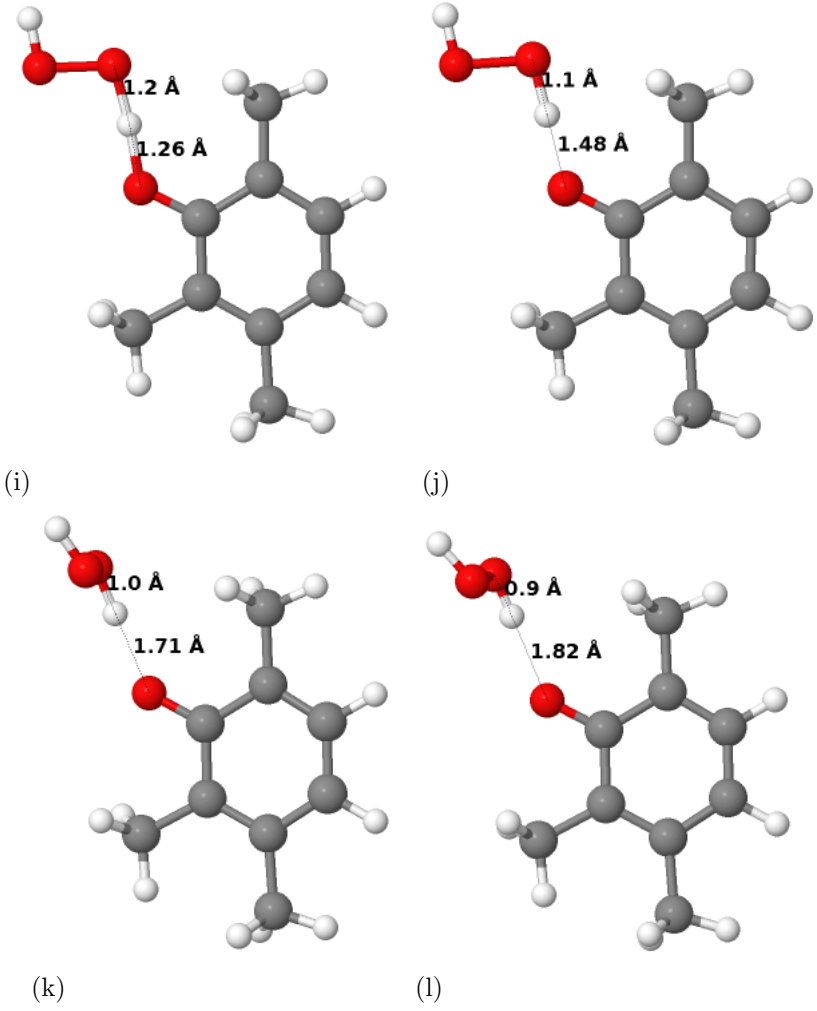

Figure B.1: *Geometries for the hydrogen transfer from simplification B to $^{\bullet}OOH$ seen in figure 4.8. The hydrogen bond length between the hydrogen atom in the hydroxyl group and the oxygen in the radical is (i) 1,20 Å, (j) 1,10 Å, (k) 1,00 Å, and (l) 0,90 Å.*

Appendix C

Imaginary frequencies for transition states

To validate that the real transition states are found throughout this thesis, figure C.1-C.5 shows the imaginary frequencies. The arrow shows the main feature of the normal mode for the imaginary frequency.

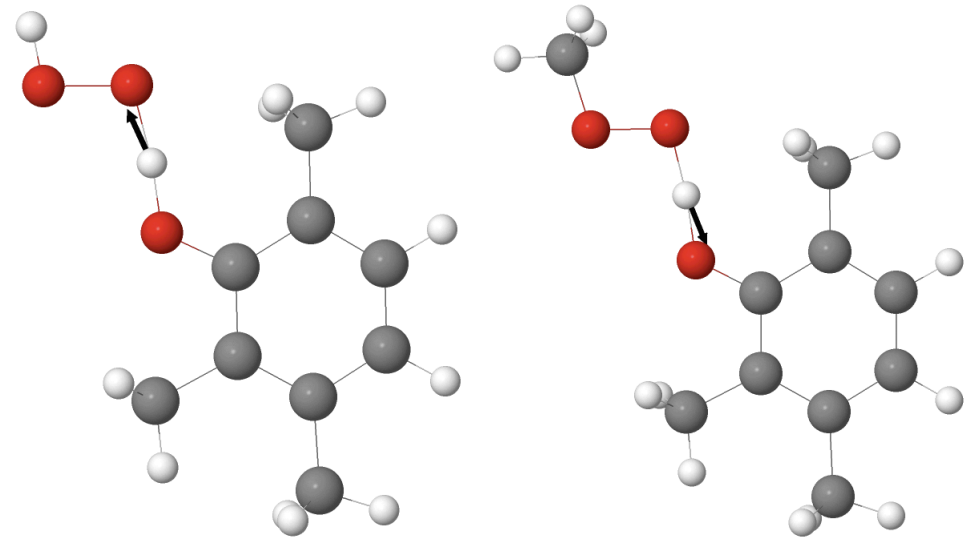

(a)

(b)

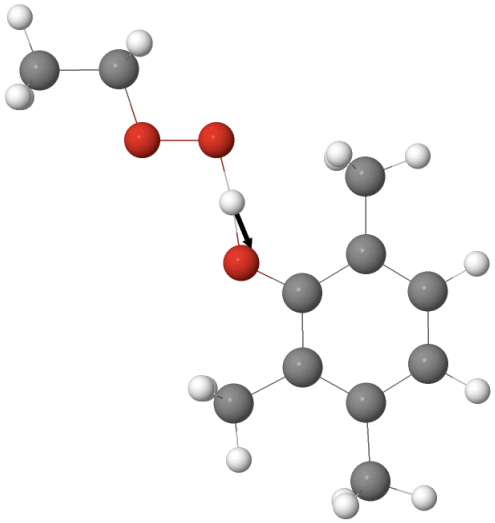

(c)

Figure C.1: *Imaginary frequencies for simplification* **B** *hydrogen bonded to hydroperoxide radicals. (a)* $^{\bullet}OOH$*: -962* cm^{-1}*. (b)* $^{\bullet}OOCH_3$*: -1107* cm^{-1}*. (c)* $^{\bullet}OOC_2H_5$*: -1133* cm^{-1}*.*

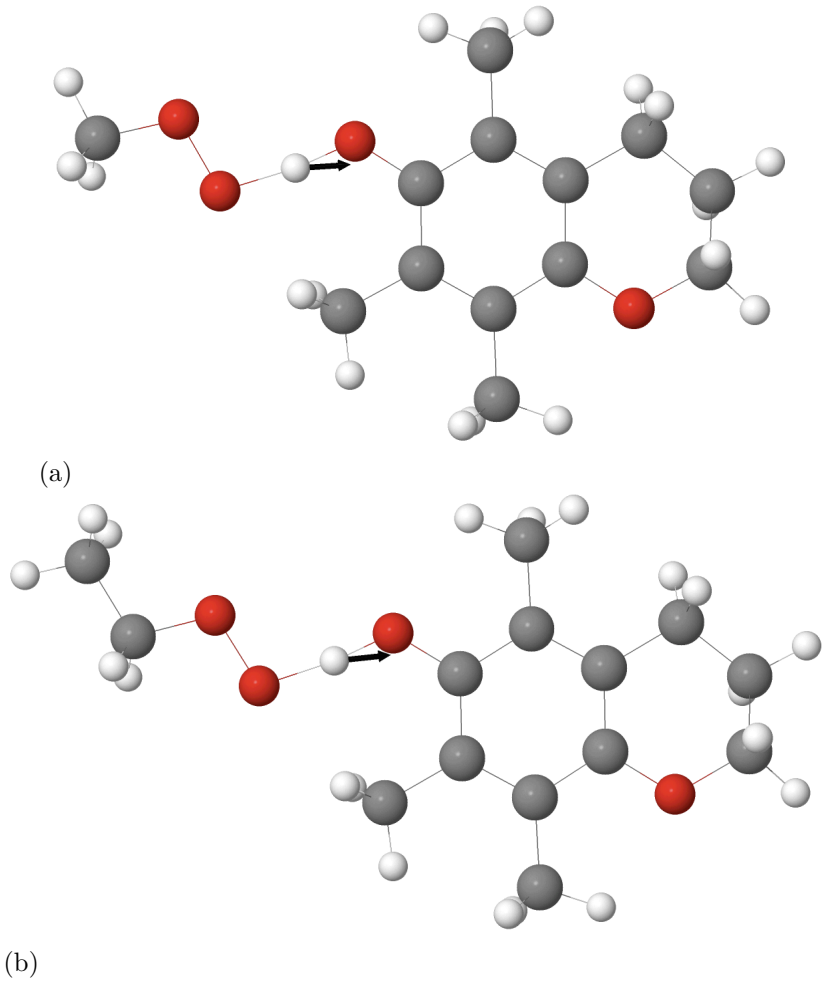

Figure C.2: *Imaginary frequencies for simplification* **A** *hydrogen bonded to hydroperoxide radicals. (a)* $^{\bullet}OOCH_3$*: -481* cm^{-1}*. (b)* $^{\bullet}OOC_2H_5$*: -638* cm^{-1}*.*

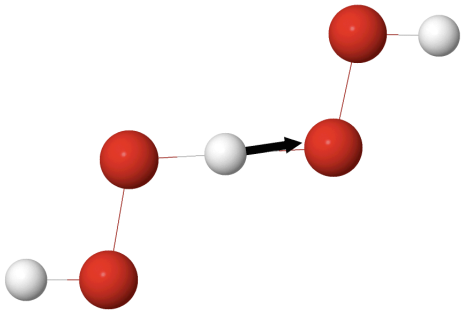

Figure C.3: *Imaginary frequencies for transition state for hydrogen transfer from HOOH to* $^{\bullet}OOH$*. -1192* cm^{-1}*.*

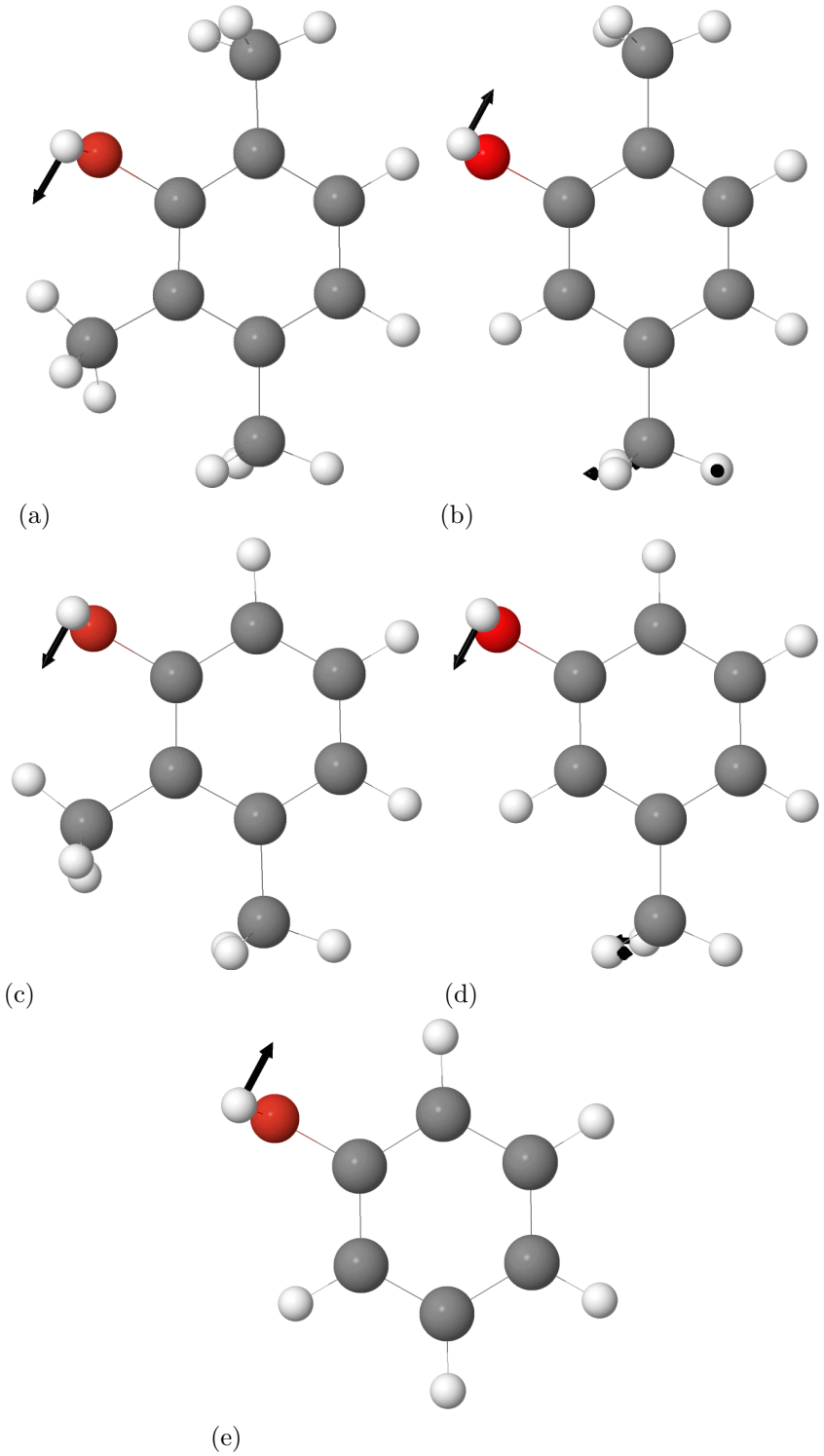

Figure C.4: *Imaginary frequency for the transition state for rotation of the hydroxyl group on the five isoforms of simplification* **B**. *(a) α-isoform -309 cm^{-1} (b) β-isoform -348 cm^{-1} -59 cm^{-1} (c) γ-isoform -308 cm^{-1} (d) δ-isoform -338 cm^{-1} -48 cm^{-1} (e) Isoform without methyl groups -340 cm^{-1}.*

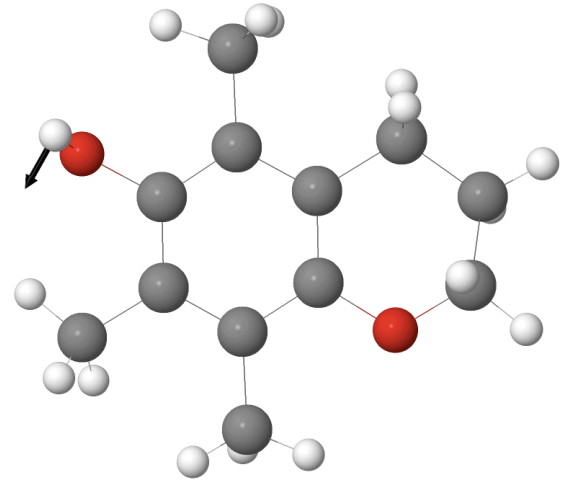

(a)

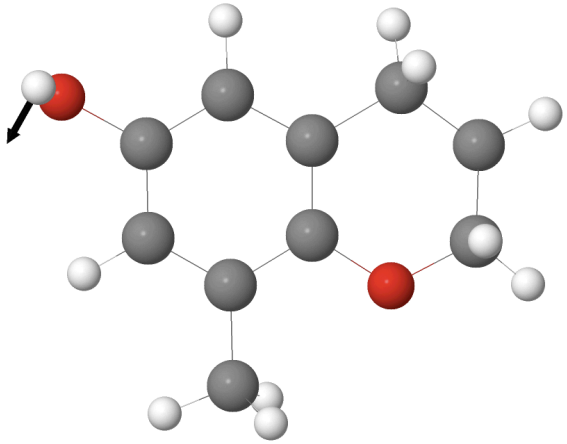

(b)

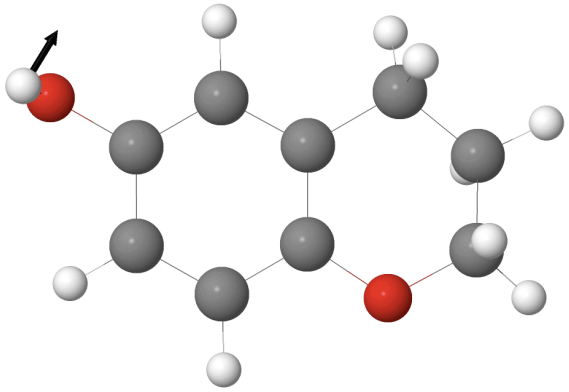

(c)

Figure C.5: *Imaginary frequency for the transition state for rotation of the hydroxyl group on the five isoforms of simplification* **A**. *(a) α-isoform -219 cm^{-1} (b) δ-isoform -303 cm^{-1} (c) Isoform without methyl groups -294 cm^{-1}.*